Wear Behaviour of Thermally Sprayed Metallic and Ceramic Coatings

by

Saifi Usmani

A thesis
presented to the University of Manitoba
in fulfilment of the
thesis requirement for the degree of
Master of Science
in
Mechanical and Industrial Engineering

Winnipeg, Manitoba, Canada 1992

ISBN 0-315-77711-7

WEAR BEHAVIOUR OF THERMALLY SPRAYED METALLIC AND CERAMIC COATINGS

BY

SAIFI USMANI

A Thesis submitted to the Faculty of Graduate Studies of the University of Manitoba in partial fulfillment of the requirements for the degree of

MASTER OF SCIENCE

DEDICATION

I dedicate this thesis to Ammu, Mummy and Hapu. They are that I am.

ABSTRACT

A wear test apparatus was built to simulate the wear conditions in a diesel engine cylinder liner. The apparatus was designed to conduct lubricated and unlubricated, reciprocating, sliding wear tests under conditions of low to high temperature. This apparatus was used to conduct unlubricated wear tests on three specimens, with an arc-sprayed martensitic stainless steel coating. These tests, conducted under the same operating and surface conditions, produced comparative results between the three specimens and revealed the occurrence of the same sequence of wear as in metals. Furthermore, comparative lubricated wear tests on three coatings indicate the similarity in the performance of plasma-sprayed Cr_2O_3 and electroplated chromium, for application in diesel engine liners. The beneficial effects of a porous surface, in this context, have been discussed.

ACKNOWLEDGEMENTS

I wish to express my sincere gratitude to my supervisor, Dr. Kedar Nath Tandon for his deep interest and guidance throughout the preparation of this thesis and to Transport Development Centre, Transport Canada, Montreal, PQ for the financial support for my M.Sc program. I would also like to thank M/S Don Mardis, John Van Dorp, Ron Crampton and Lincoln Oree for their technical help. I am grateful to Prof. J. R. Cahoon for his useful suggestions during various stages of this research.

Among my friends, the support and assistance of Om, Takyi and Kwame has been invaluable to me. I am glad that I have such good friends.

Finally, I will acknowledge the assistance of and consultations with my various laboratory colleagues.

Contents

List of Tables

List of Figures

Chapter 1

OBJECTIVES AND SCOPE

This chapter discusses the objectives and the scope of this thesis.

1.1 The Objectives

The objectives of this thesis can be classified under three categories:

1. Test Methods: To design and fabricate a wear test apparatus.

2. Dry Tests:To study the progression of wear during unlubricated, reciprocating, sliding wear of arc-sprayed martensitic stainless steel. Simultaneously, to evaluate the reproducibility of the wear test apparatus.

3. Comparative Tests:To evaluate and compare the performance of three coatings for wear resistant applications in diesel engine liners. Consequently, to evaluate chrome-plating, plasma-sprayed chromium oxide, and arc-sprayed martensitic stainless steel coatings under conditions of medium temperature, lubricated, reciprocating, sliding wear.

Hereafter, these objectives shall be referred to as test methods, dry tests, and comparative tests respectively.

1.2 The Scope

The scope of this thesis encompasses five additional chapters, the contents of which are discussed here. The first of these includes an introduction to the process of chrome-plating in diesel engine liners, the problems therein and the alternatives to the process. In the same chapter, a group of alternatives to chrome-plating, the research already conducted on these and the need for further research is briefly discussed. In the following chapter, a background of the approaches to characterization of materials in wear resistant applications, alongwith other characterization techniques, is presented. The rest of the thesis deals with work actually conducted as part of the present research. The development of a wear testing apparatus, selection of wear quantification schemes, and physical characterization techniques, used in this work are discussed in chapter 4; the results and deductions from them in chapter 5; and conclusions in chapter 6. The various scientific articles referred to in this work are listed at the end, under the heading references.

Chapter 2

INTRODUCTION

In this chapter, alternatives to chrome-plating, as a wear resistant surface in diesel engine liners, are discussed. Consequently, the process of thermal spraying, the research already conducted on the evaluation of thermally sprayed coatings, and the need for further research on them are also discussed.

2.1 Wear In Diesel Engine Liners

Wear in diesel engine liners can vary over a wide range. It has been claimed [1] that wear on the diameter in a cylinder can vary from 0.15 mm to 3.0 mm per thousand hours of operation, and that corrosion and scuffing (defined on page 15) are the two major causes of it. Initial measures taken to control such wear were the use of austenitic iron as, and the addition of vanadium in the composition of, cylinder liner material [1, 2]. Further surface treatments involved the use of chromium plated liners.

The process of chromium plating has, however, certain inherent shortcomings. It has the problems of peeling-off under severe operating conditions [2], stress cracking [3, 4], and expensive post-plating treatment [4]. Moreover, chromium plating is a slow process and entails the disposition of hazardous chemicals from the process into the environment [5]. It also depends on the supply of chromium which is a strategic metal, its supply dependent on the world political situation [6]. Hence, alternatives to this process are being investigated. Thermal spraying is one of them.

2.2 Thermal Spraying

Thermal spraying is a process by which a heat source is used to melt and sometimes propel coating material onto a prepared substrate surface where it solidifies to give a coating. A variety of heat sources and materials are used in this process to give a large variety of coated surfaces [7]-[11]. Plasma-spraying and arc-spraying are two main thermal spraying processes. Schematic diagrams of the spraying equipment involved in these two processes [8, 12], are given in Figure 2.1. Other details of the processes are available in the literature [8, 12, 13]. Overall, this process is much faster and versatile than chrome-plating.

The coatings produced by thermal spraying have a splat like structure. This kind of structure as described recently [8] for the case of plasma-sprayed coatings is shown in Figure 2.2: Splats result from the spreading out and splattering of the molten coating material particles, some of them oxidized during their travel from the nozzle of the spray gun to the substrate surface. As this deposit grows into a coating, it traps air, which results in voids. The thickness of this deposit may vary as required for a certain application, but, generally thermally sprayed coatings are thick (greater than 10μm) and are different from other surface treatments like thin film processes, in which very little, if any, mass is added to the surface.

The quality of these coatings depends on many process parameters [9, 14, 15]. Some of the more than fifty process parameters claimed [9], for example, to affect the quality of plasma-sprayed coatings are given in Figure 2.3.

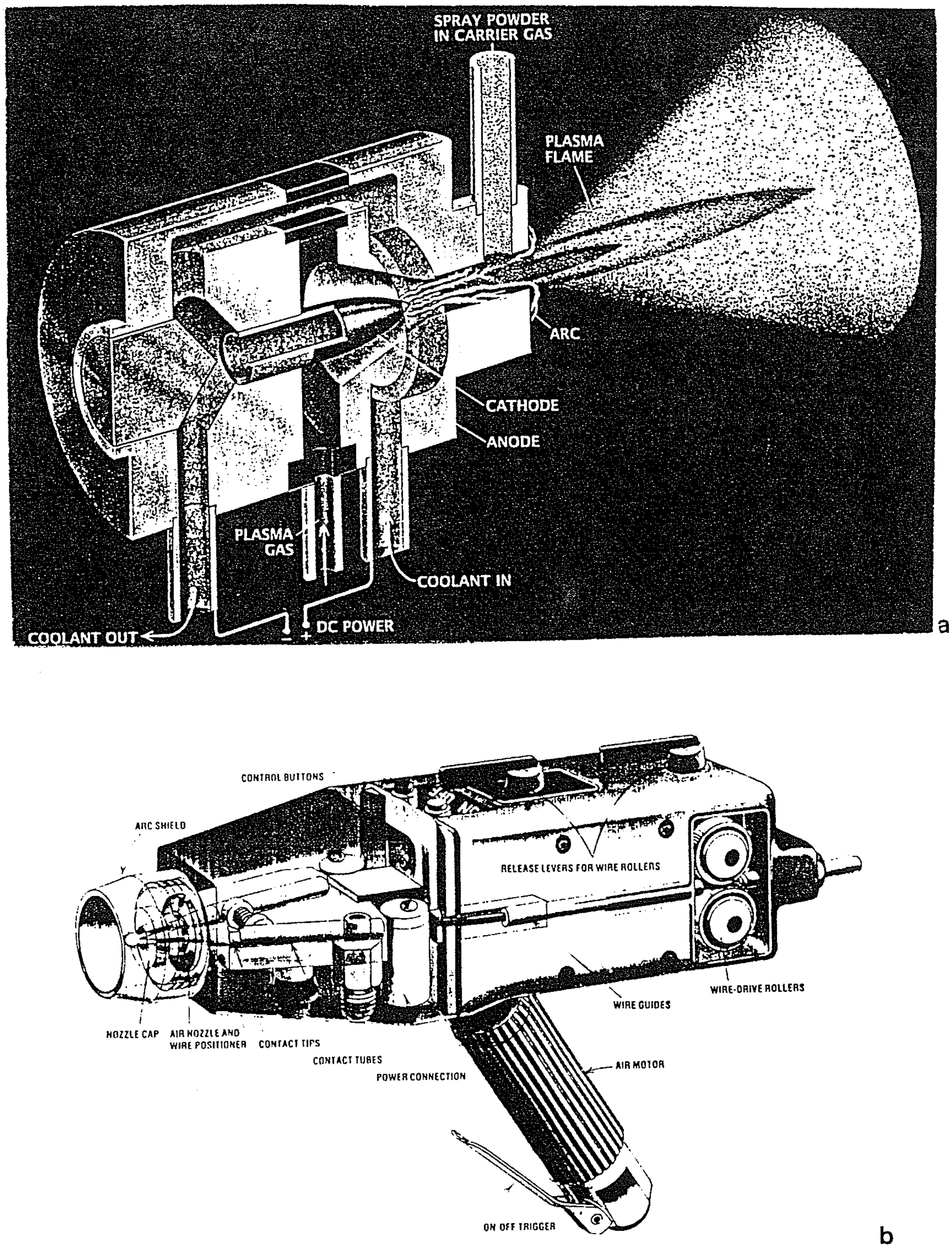

Figure 2.1: a: Plasma-spray, [8] and b: arc-spray equipment [12]

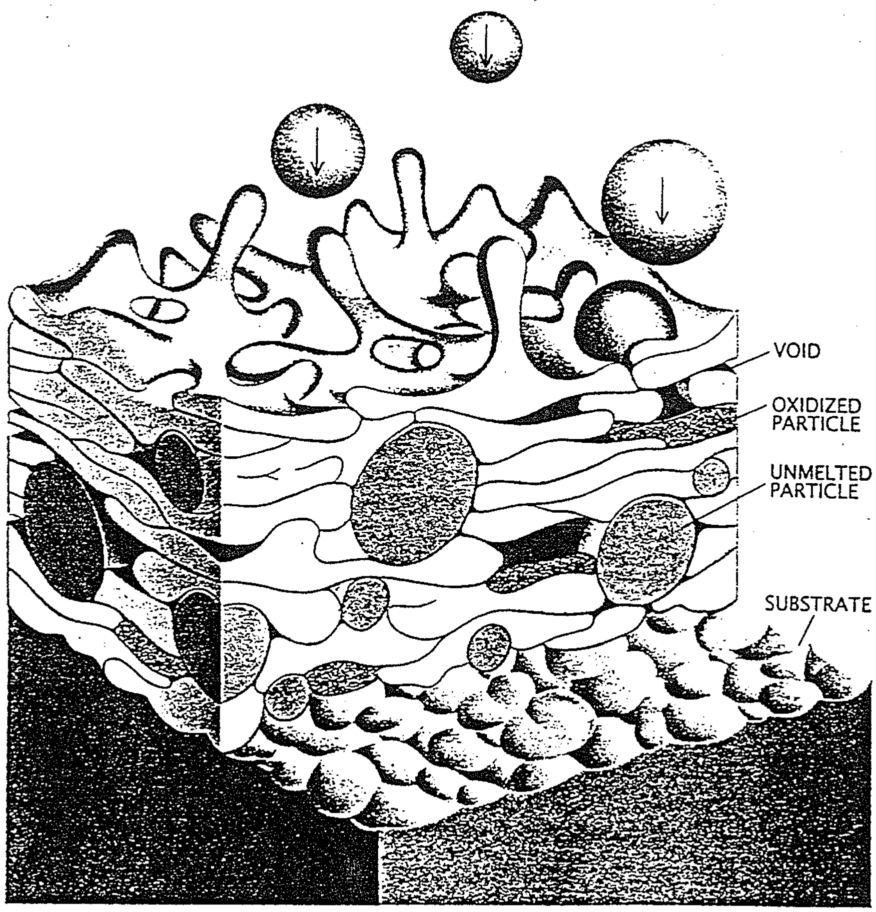

Figure 2.2: Buildup of thermally sprayed coating [8]

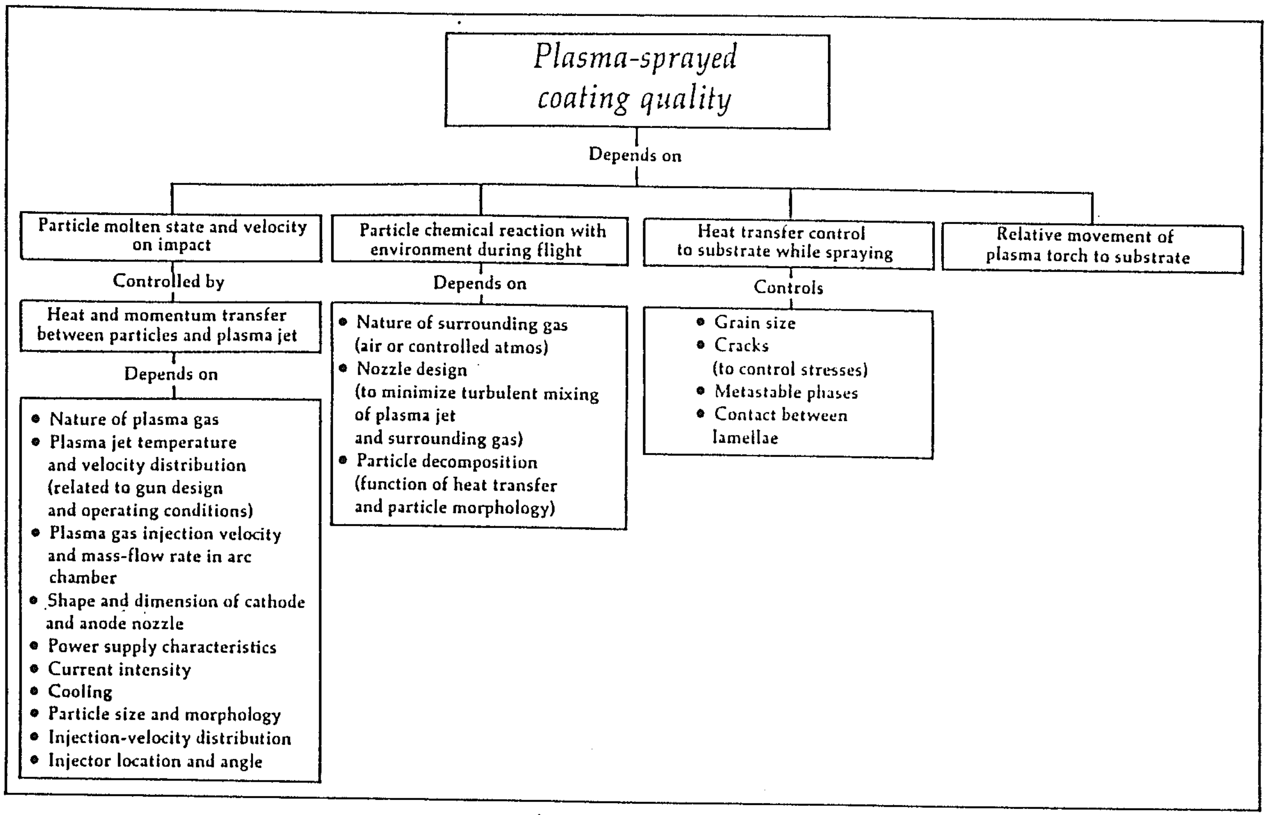

Figure 2.3: Process parameters known to affect coating quality [9]

The major factors which control the structure of a particular coating are the temperature, velocity and size distribution of the incident particles, since coatings are formed by the impact of a stream of particles striking the substrate [14]. Moreover, rapid heating and cooling of the substrate and the coating results in an extremely fine crystal size of the sprayed deposit, or in certain cases amorphous or partly amorphous structures [14], and has been found to promote large thermal stresses in the coatings [15].

Recently, an increased control in the quality of the coatings has been possible because of increased sophistication of coating-application equipment, common use of mass-flow gas controllers and meters, and improved quality and control of feedstock consumables [7]. Coating technology has advanced tremendously since its inception and there is a large and well established literature on the subject of coatings, coating processes, and coating characterization. Still, it is imperative to characterize the coatings for each specialized application in order to ensure that an optimum performance can be achieved.

2.3 Scope of Research

The purpose of this work was to conduct fundamental research which could benefit the evaluation and application of thermally sprayed coatings in wear resistant applications. Moreover, this work can complement other work available on the subjects covered here. It is hoped that a combination of research by different investigators shall give a wider understanding of the wear phenomena in thermally sprayed coatings.

To avoid overlap of research work, an extensive survey of the available literature on the subject of ceramic and metallic surfaces, bulk, thermally sprayed, or deposited by other means onto substrates, was undertaken. The information found on wear characterization [16]-[23], bond strength testing [12, 16, 18], microscopy, and structure-property relationship studies of chromium electrodeposits [3] and on other thermally sprayed coatings [24] was overwhelming. However, research on the progression of wear under unlubricated conditions and characterization under lubricated, reciprocating, sliding wear conditions, of the selected coatings was found to be lacking. Hence, the the dry tests and the comparative tests were formulated, in an attempt to accomplish some of this missing work.

Consequently, in the present work, the progression of wear of martensitic stainless steel (AS–0.3%C, 13.5% Cr) under unlubricated, reciprocating, sliding wear conditions was studied. Moreover, the lubricated, reciprocating, sliding wear performance of martensitic stainless steel (AS–0.3%C, 13.5% Cr), and plasma-sprayed Cr_2O_3 (PC) was compared with that of electrochemically deposited chromium (EC). The sliding material against all the surfaces in both lubricated and unlubricated wear tests was martensitic nodular cast iron (CI). Hereafter, the terms AS, PC, EC and CI shall be used to refer to the respective materials or specimens. The sprayed coatings were selected for evaluation because stainless steel has been claimed to be an all-purpose wear-resistant material [25], and Cr_2O_3 based coatings deposited using other processes have performed well in some wear tests [16, 18]. In addition to this, bond strength testing and microstructural characterization of the coatings was performed.

In order to better understand the wear performance of the coatings, a background knowledge on the subject of wear can be very helpful. This issue is addressed next.

Chapter 3

LITERATURE REVIEW

In this chapter, various wear classification schemes, test methodologies and approaches to wear quantification have been discussed. Simultaneously, material characterization techniques and other relevant material has been discussed. The concepts discussed below may be essential in understanding some of the work in the chapters to follow.

3.1 Wear Characterization

Wear, along with friction and lubrication, forms the subject of Tribology which is defined as "the science and technology of interacting surfaces in relative motion and of related subjects and practices" [26, 27]. All the aspects of tribology, including wear, constitute a very complex subject. The problem is further complicated because wear is a property of the system [27]; that is, it depends as much on the imposed sliding conditions as on the properties of the materials concerned. Nevertheless, there have been numerous attempts at developing a formal classification of wear processes. The three factors that are considered [28] to be the most important for such a work are "a. an adequate definition of wear, b. the identification and classification of different unique mechanisms by which wear occurs, and c. the use of a standard test device to accumulate a collective body of knowledge."

3.2 Definition of Wear

As regards the first of the three requirements stated-above, there seems to be some agreement and wear is generally defined as: the "unwanted removal of material by chemical or mechanical action [28]." This definition is only an approximation because in certain cases plastic flow may occur, and, for all practical purposes, wear has occurred even though no material has been removed. This omission appears to have been redressed in a recent definition of wear "as displacement or removal of material as a result of tribological processes" [29].

3.3 Classification of Wear Processes

3.3.1 Conventional Classification Schemes

The classification of the various wear processes is a very difficult task. "Conventionally," wear classification schemes have been based on terminology which emphasizes an assumed mechanism. Examples are such terms as abrasion, adhesive wear, erosion and fatigue wear. These mechanisms can be further divided into different categories, such as the division of abrasion wear mechanism into low stress, high stress, gouging, and polishing [30]; and cutting, flaking, wedge formation and ploughing [31]. Moreover, sometimes several names describe one mechanism; sometimes, one term is used to describe wear which results from several processes acting together or in a sequence. Furthermore, the consequences of the various wear mechanisms on different materials will be governed by the properties of the respective materials. For example, abrasion might have varying consequences on different materials (Figure 3.1, source [32]).

Thus, although the classification of wear is linked to the mechanisms by which it occurs, the use of a very large number of terms to describe the wear mechanisms presents a confusing picture. Recently however, there has been an attempt to reduce all wear processes into four categories based on commonality of mechanism [30], Figure 3.2.

A listing of the descriptions of some of the wear mechanisms from this figure, more commonly encountered, is not out of order here:

Abrasion: Wear produced by hard particles or protuberances forced against and moving along a solid surface.

Adhesive Wear: Progressive loss of material from solid surfaces in relative motion that is at least initiated by localized bonding between these surfaces.

Erosion/Corrosion: Progressive loss of original material from a solid surface due to the mechanical interaction between that surface and a fluid or impinging fluid stream.

Surface Fatigue: Fracture of material from a solid surface caused by the cyclic stresses produced by repeated rolling or sliding on a surface. The prime manifestation of surface fatigue is in the form of **pitting wear**. In this type of wear, repeated sliding or rolling causes subsurface cracks that grow to produce a fracture of a local area of the surface.

Polishing Wear: Progressive removal of material from a surface by the action of rubbing from other solids under such conditions that material from a surface is removed without visible scratching, fracture, or plastic deformation of the surface.

Seizure: The stopping of relative motion as a result of interfacial friction. Local solid-state welding may be part of the mechanism of seizure.

Material	Deformation mode	Particle detachment processes	Material properties
Metals	Plastic–elastic	Plastic grooving Prow formation Cutting (chip formation)	Hardness Ductility
Polymers	Elastic–plastic	Plastic grooving Cutting Fatigue	Toughness (*se*) Fatigue properties
Elastomers	Elastic	Tearing Roll formation Fatigue	Tensile strength Elastic modulus Fatigue properties
Ceramics (carbons)	Elastic Brittle fracture	Crack propagation Flaking Fatigue	H/E ratio Fracture toughness

Figure 3.1: Materials aspects of abrasive wear [32]

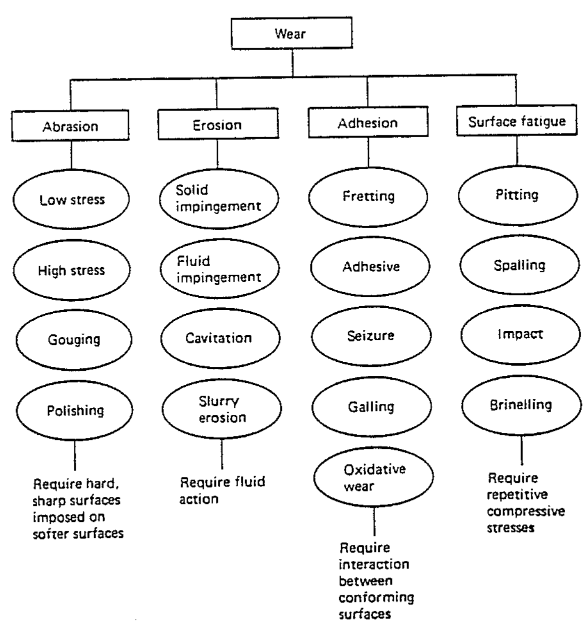

Figure 3.2: The categories of wear [30]

Among the mechanisms defined above, three mechanisms, of much relevance to the dry tests, need some elaboration. These are pitting wear, abrasive wear and adhesive wear.

Pitting or delamination wear are very common modes of debris production in cases of cyclic loading, as in sliding wear. It has been claimed [37] that under the conditions of high contact pressure, at low sliding velocities, the resultant frictional traction causes a catastrophic increase in the plastic shear strain accumulated in the subsurface layer. This is where cracks nucleate and grow parallel to the surface, eventually breaking out to give flake-like debris.

In abrasive wear, large wear debris leads to surface roughening and further ploughing action, giving high wear rates. A model developed to explain this is presented in Figure 3.3 [35].

Adhesive wear is considered to be the initiation mode of almost all dry sliding wear systems, but as wear progresses it becomes mixed mode [30]. Hence, a surface subjected to adhesive wear can have many different appearances. During adhesion, if the bond to one surface is stronger than the bond to the other, transfer of material may occur. Else, if surface features are fractured from both surfaces, wear debris is formed. Moreover, plastic deformation of surface asperities may also occur. The concept of wearing away of surface asperities due to frictional heating has been dealt with in a recent review [33].

The concept of relative rest between two surfaces, during adhesive wear, can, however, generate much heated debate [34]. Three different mechanisms have been suggested: (1) local cold welding, especially at cracks in surface films, (2) the presence of some "sticky" interfacial material, and (3) mechanical interlocking of surfaces (Figure 3.4). Having, discussed this view, a model on adhesive wear (seizure) is presented here. In this model (Figure 3.5, [35]), large wear debris is thought either to transfer to the pin or trapped between the sliding interfaces. In either case, during the sliding process, a wedge is formed and stick-slip motion occurs. Regarding slip motion, it is claimed that [38] three different types of slip motions may occur (Figure 3.6).

Basically, slip occurs once the wedge is overcome or the debris is separated. At this stage, the sliding component moves up and down and vibration occurs. This, alongwith a sudden increase in noise, is described [36] as a manifestation of scuffing wear.

Scuffing wear is a severe form of wear and invariably leads to seizure of the sliding components. It may produce scoring, a series of grooves and ridges in the surface oriented in the sliding direction, possibly accompanied by a metallurgical transformation [36]. However, the surfaces are completely non-directional in appearance. The scoring is thought to be caused by the abrasive and adhesive wear preceding scuffing. It has been claimed that abrasive wear precedes adhesive wear [35] and that either pitting or mild adhesive wear precede scuffing [36]. In either of the preceding mechanisms, debris production is a notable feature. Hence, it can be assumed that the presence of wear debris may be a cause of scuffing. The presence of wear debris between the sliding interfaces has, also, been found to generate high friction [23], during repeat pass sliding of ceramics. This may explain the abrupt rise of friction during scuffing. Although such a rise in friction is another prime manifestation of scuffing, it is not sure whether it is the cause or effect of scuffing [36].

3.3.2 Recent Classification Schemes

In a recent work [32], some of the above mentioned wear mechanisms: abrasion, adhesion, fatigue and corrosion, have been identified as the principal wear mechanisms in particle detachment and debris production processes—one of the recent approaches to wear classification [29, 32, 37]. However, in this approach deformation and chemical

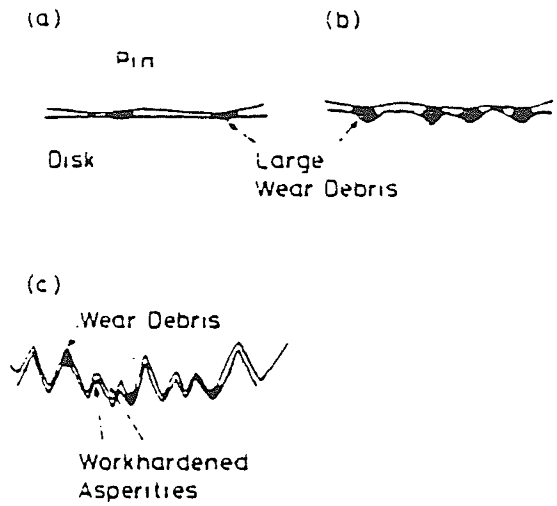

Figure 3.3: Abrasive wear model [35]

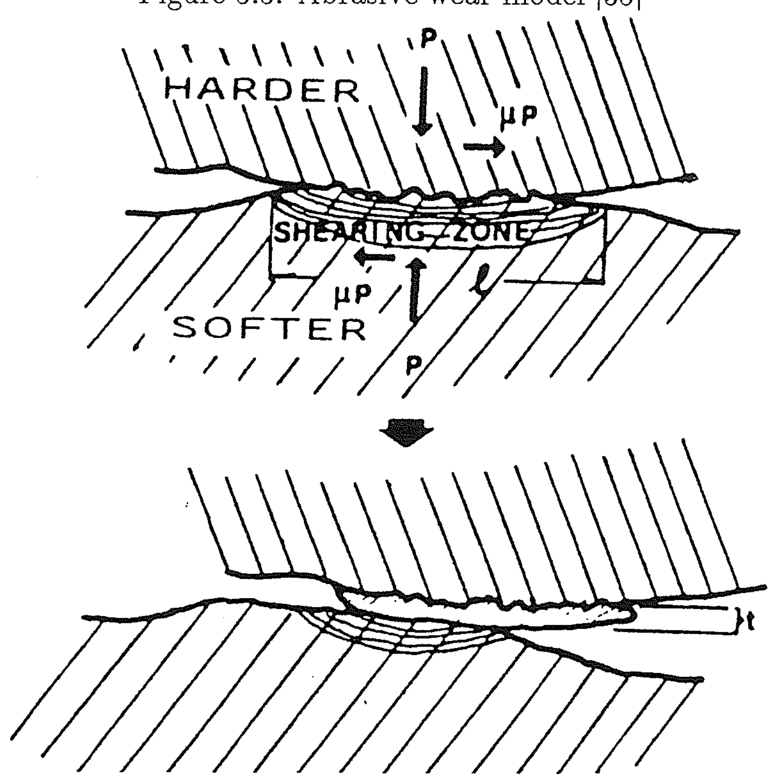

Figure 3.4: Model of relative rest due to mechanical interlocking [34]

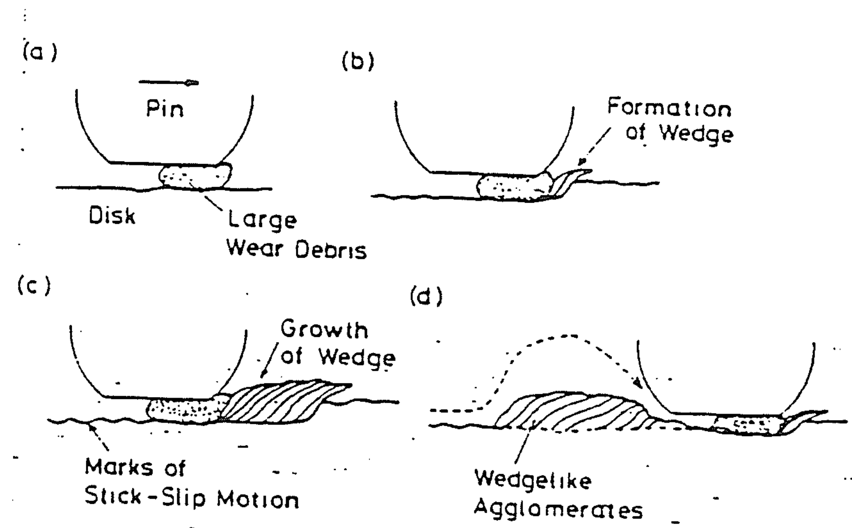

Figure 3.5: Adhesive wear model [35]

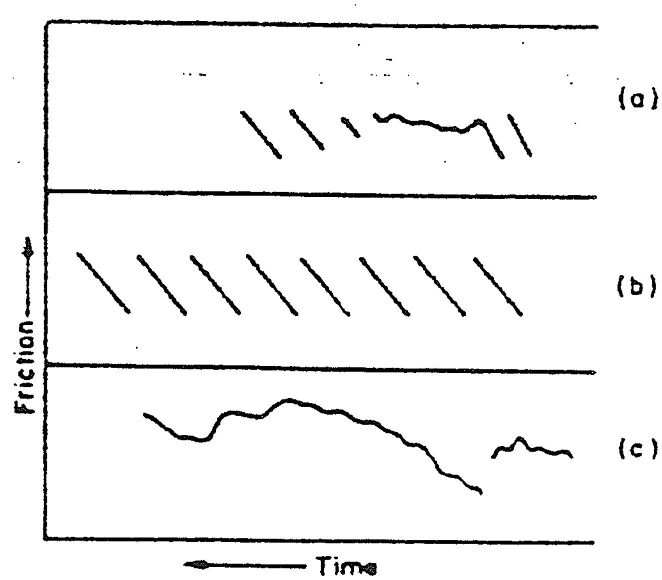

Figure 3.6: Types of slip motions during stick-slip [38] (a) Hard pin on soft surfaces; (b) Soft pin on hard surfaces; and (c) Similar metals

attack between the generation and analysis of the particles is possible and it may influence the deductions unless debris collection takes place as soon as possible after generation [34]. In order to circumvent this problem, another investigator [32] believes that a classification scheme based primarily on the mechanisms by which particles are detached, coupled with details on how specific geometrical arrangements then respond in producing debris, is a more reliable and far-sighted approach. This scheme is still in its developmental stage.

Meanwhile, an approach previously used for the construction of wear-mechanism maps by plotting the data from various wear experiments on suitable axes (F/A_n and v, for example [35]) and identifying the wear rate and mechanism, has been modified [29, 39] to include a more general classification scheme based on the classical "mild" and "severe" classification [40]. In the "new" approach instead of identifying each mechanism, only the dominant mechanism is identified. Examples of the two approaches are given in Figure 3.7 [41]. Depending on the sliding conditions the transitions between mild and severe wear take place over a wide range. These transitions are of two broad types: those which are load-dependent and those which are velocity dependent. In addition, a third transition—sliding-distance dependant—is also found. Examples are given in Figure 3.8.

3.4 Lubrication

With respect to the last approach described above, it must be pointed out that the examples do not yet include lubricated wear results. This might limit the application of these maps since lubrication may influence the rate of wear and the apppearance or progression of wear mechanisms dramatically. This can be caused by influencing surface energies, causing oxides or other layers to form, or affecting the degree of contact between the two surfaces, depending on the thickness of the lubricant film

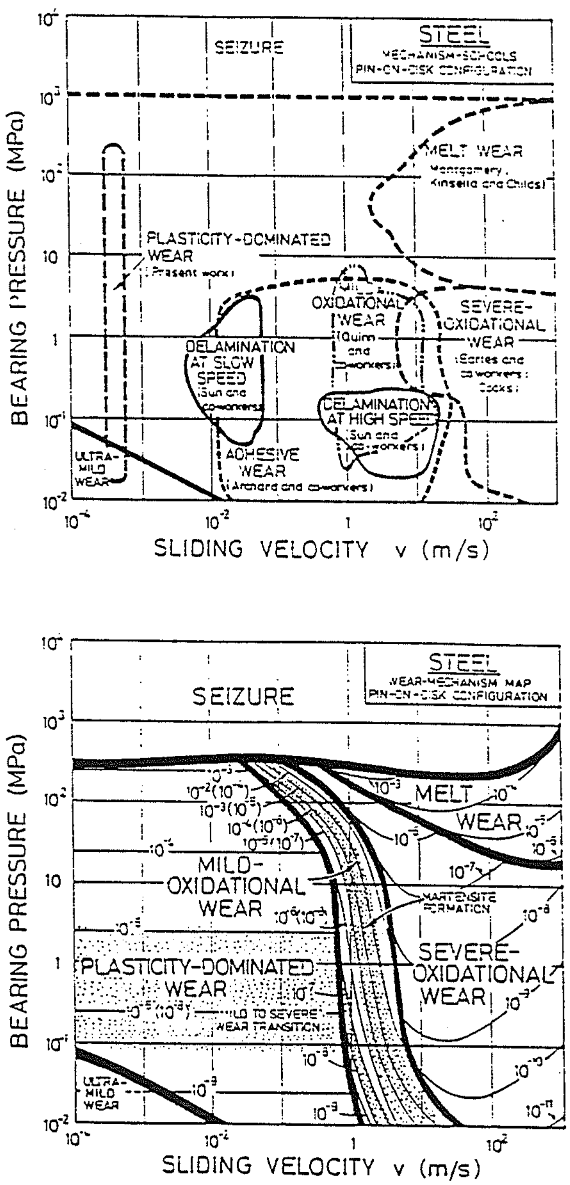

Figure 3.7: Wear mechanism maps–a:individual mechanisms identified, and b: only the dominant mechanism identified [41]

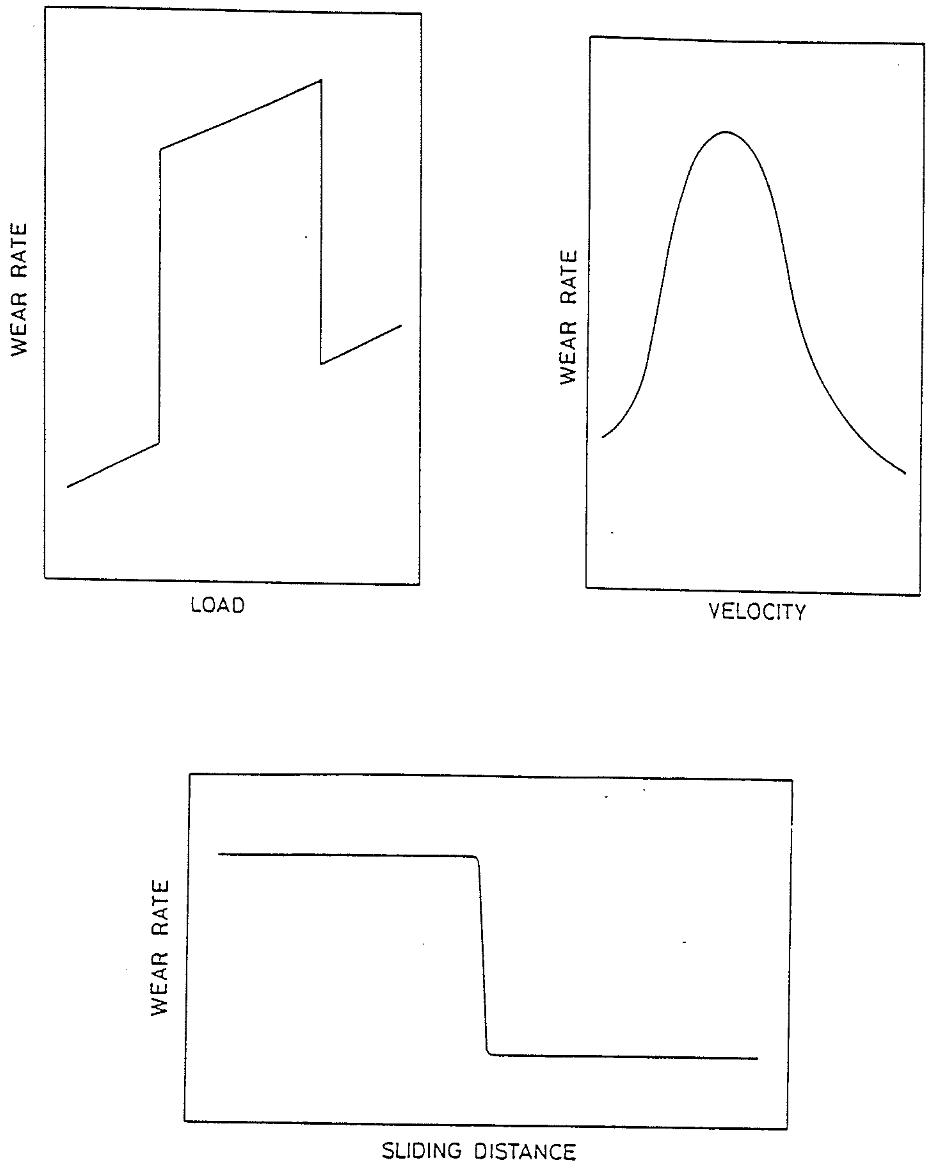

Figure 3.8: Wear mechanism transitions [37]

[42]. The thickness of this film may vary depending on the relative speeds, contact geometry, and loading conditions. Consequently, a variety of lubrication regimes such as those shown in Figure 3.9 [42] are possible. Specifically, hydrodynamic lubrication at high speeds and low loads and boundary lubrication at low velocities and high loads are possible [21].

The wear mechanisms under these regimes may then undergo a change in their description as opposed to that under unlubricated wear. Such a modified description, as found in the literature [43, 44], has been presented here for four mechanisms:

Adhesive wear: occurs under lubricated conditions when the hydrodynamic or elastohydrodynamic film is so thin that surface asperities penetrate the film.

Corrosive chemical wear: Antiwear or extreme pressure additives generally function by chemical reaction with surfaces. During relative motion of surfaces, some reaction product is lost by shearing or mechanical action giving rise to chemical wear.

Abrasive wear: results from a cutting action by (1) a rough, hard surface sliding against a softer surface, or (2) contaminant hard particles trapped between sliding surfaces. Hydrodynamic, or elastohydrodynamic, lubricant films either sufficiently thick to separate the surfaces in (1) or thicker than the largest hard particles in (2) will greatly reduce abrasive wear.

Contact fatigue: contaminant hard particles in the lubricant can act as stress initiators for surface microcracks, leading to spalling or pitting forms of fatigue wear.

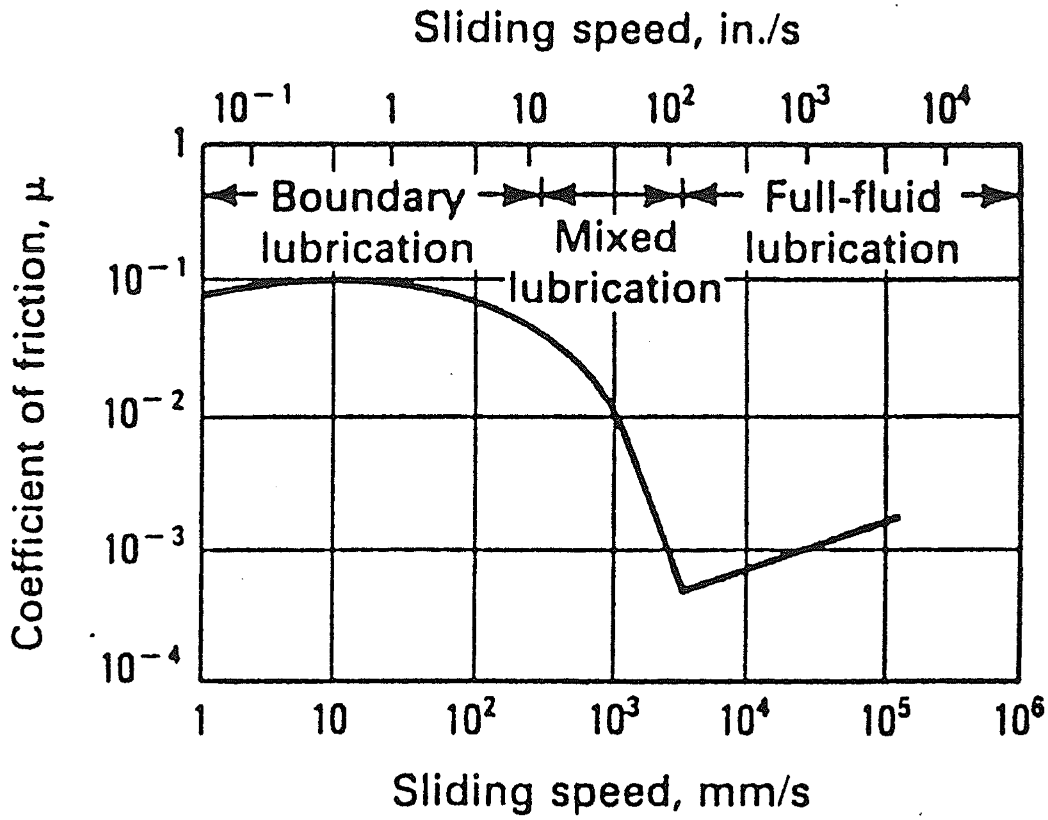

Figure 3.9: Lubrication regimes [42]

It has been claimed in a study on the wear of carbon steel [35] that, the predominant wear mechanisms in lubricated sliding friction are flow wear, abrasive wear (ploughing) and adhesive wear. In the case of lubricated wear of cylinder-ring combination in a diesel engine liner, the wear is thought to proceed in the following sequence [45]:

1. The Break-in stage: Excessive surface damage at this stage is often referred to as scuffing but it is not uniquely described by this term.

2. The Progressive wear stage: The wear of cylinder in this stage may occur by several mechanisms but mostly by abrasion and corrosion.

3. A catastrophic mechanism: due to unusual events, such as high temperature, high loads, interruptions of oil supply or intake of large quantity of contaminants, widely referred to as scuffing.

To reduce the catastrophic wear mechanism, the importance of uncontaminated liquid lubricants needs be emphasized here. Such lubricants scavenge wear debris and remove heat from contacting surfaces. The latter reduces operating temperature, resulting in the formation of thicker oil films and/or a lower demand on the lubricant additives. Scavenging of the wear debris lessens the chance of interaction of small wear particles to form larger, work-hardened particles which can cause abrasive wear, higher surface temperatures, and mechanical destruction of the surface anti-wear film [43].

Before we end this sub-section it must be pointed out that in all the classifications discussed above, a great degree of personal judgment is involved [46]. A suggestion for a possible minimization of this effect involves a two-part procedure. The first part involves the examination of the loading to see whether it is predominantly shear or normal, the second constituting the carrying out of a series of wear tests and determining the dependence of the wear rate on the relevant variables [46]. Hence, the next important issue is that of wear tests, and variables.

3.5 Wear Testing

The majority of wear tests are carried out between unlubricated surfaces [33]. The reasons are two-fold. First, the wear of well lubricated systems is extremely small and experimental studies would be long, tedious, and probably irreproducible because wear is dependent on a variety of factors. Secondly, it is tacitly asssumed that wear occurs primarily as a result of lubricant breakdown and that local lubricant breakdown is equaivalent to dry contact. Thus, selection of wear tests can be made depending upon the wear testing requirements .

Wear tests can be designed to study one of the following four categories: fundamental understanding, determination of the effect of variables, characterization of materials and lubricants, and selection of materials for a specific application. In the first two categories, the type of test rig is less important than how it is used or what information is gathered and what is now needed, whereas in the last two categories, the type of test rig is important [17]. Thus, depending upon the requirement, many types of standardized and non-standardized wear tests exist; from small lab-scale tests that attempt to evaluate general performance to full-size models designed to measure performance in a specific application [47].

Currently, standardized methods for tribotesting are being evaluated in round-robin tests under the Versailles Project on Advanced Materials and Standards (VAMAS), as a means of: "a. improvement of the reproducibility and compatibility of wear tests by developing internationally agreed wear test methodologies, and b. characterization of the wear behaviour of "advanced materials" in comparison with conventional methods [48]." At present, the VAMAS testing program involves the dry sliding, wear and friction tests on a ball-on-disc configuration.

Examples of other standardized wear test methods include the block-on-ring test, ASTM G77 [49], crossed cylinder-on-cylinder test, ASTM G83 [50], and the pin-on-disk test, ASTM G99 [51]. The first two test geometries are for non-lubricated testing, whereas in the third case lubricants and contaminants can be present as well. In all the standard test methods, the specimen geometry and size, and the usual test parameters are carefully specified; the operating parameters - load and/or speed - are controlled to simulate those encountered in the application. Repeatability of these standard tests, for the non-lubricated, non-abrasive case, as catalogued in literature [52], has not been found to be good (Figure 3.10). Hence, these tests are useful for comparing relative wear resistance of materials for screening purposes or for quality control, rather than for predicting actual wear in a new application [47, 50, 51].

Test method	*Materials*	*Conditions*	*Coefficient of variation within-laboratory, total volume loss (%)*
Cylinder/cylinder (G-83 std.) [9]	M2 steel/M2 steel	71 N load; 0.266 m s^{-1}; 3190 m; lab air	31
			15
	M4 steel/M4 steel		19
			19
		Average	21
Block/ring (G-77 std.) [10]	01 steel/ 4620 steel	134 N load; 0.13 m s^{-1}; 593 m; lab air	67
			47
		Average	57
Pin/disk (VAMAS) [3] (pin wear only)	52100 steel/ 52100 steel	10 N load; 0.1 m s^{-1}; 1000 m; lab air	12
			6
			12
			9
			12
			9
			18
			33
			6
			30
			6
			21
			9
			9
			12
			33
		Average	15
Pin/disk (U.K.) [5]	535A99 steel/ 817M40 steel	20 N load; 0.1 m s^{-1}; 1080 m; lab air	58
			38
			26
			6
			21
			33
			88
		Average	39
Abrasion (G-65 std.) [8]	D-2 steel	130 N load; 2.4 m s^{-1}; 4309 m; lab air	
		Standard	5
Erosion (G-76 std.) [11]	1020 steel	70 m s^{-1} particle velocity; 50 μm Al_2O_3; 2 g min^{-1}; air	
		Standard	4
	304 steel	Standard	5

Figure 3.10: Repeatability of standardized tests [52]

Non-standardized tests are more adaptable to simulations of specific applications, though they need to be carefully evaluated to assure that the same progression of wear occurs as in the actual application [45, 47]. In most such tests, the specimens are oriented horizontally [2, 18, 31, 35, 45, 48, 65]. In some cases the specimens are oriented vertically [19]. Both orientations have advantages and disadvantages. Other testing parameters depend on the individual testing requirements of each investigating group. More details of individual non-standardized test methods shall be provided, where needed, in the following chapters. A discussion of the various parameters that influence wear, however, is perfectly in order here.

3.5.1 Effect of Variables

In various works, it has been pointed out that the minimium porperties that need evaluation for any comprehensive work on wear are:

a. Surface properties: The nature, thickness and composition of lubricants, contaminants and surface films; the surface and interfacial energies; and the roughness or texture of the surfaces as well as the compatibility of the contacting solids in terms of shape and size [42, 46, 52].

b. Bulk properties: The structure of the materials constituting the surfaces, the tendency for molecular diffusion through the solid, the stacking fault energy and perhaps the most important of all the mechanical strength of the solids [42, 46].

c. Design parameters: Loading, type of motion, vibration, cycle time, stiffness of apparatus, etc. [42].

d. Environmental parameters: Temperature, humidity, atmosphere, etc. [42]. Hence, it appears that a proper definition and control of component and system parameters of the materials' bulk and surface conditions, thecontact geometry, and the operating and environmental conditions is required, for the reproducibility of tribological tests.

Material Parameters

Among the material bulk properties, mechanical strength, either alone or in combination with other parameters, has been found to be a major determinant of wear behaviour. The parameters representing this strength are shown to be hardness and toughness of a material [46]. It has been found that, in situations in which there is a large amount of sliding or shearing, and ductile materials are used, the rate of wear is generally governed by the Holm-Archard equation. According to this equation, wear volume V is a function of load L, the sliding distance X and hardness of the softer surface p. If the wear coefficient is referred to as k, this equation (equation 3.1) can be wriiten as:

$$V = \frac{k\ L\ X}{p} \tag{3.1}$$

It can be noted from this equation that the amount of wear is directly proportional to the energy supplied L.X and inversely proportional to the hardness p. In cases where the shearing action is moderate but the normal load is large, there is a bifurcation, with ductile materials tending to follow some adaptation of the Holm-Archard equation while brittle materials follow a law in which the wear varies as the square of the supplied energy and inversely as the square of toughness (e.g. equation 3.2).

$$V = \frac{k\ m\ \rho\ v^4}{{W_p}^2} \tag{3.2}$$

In this equation, applicable for high speed erosive wear [46], m is the total mass of the liquid, ρ the liquid density, v the velocity of the liquid and W_p the material toughness. The dependence of the wear of brittle materials on their toughness has been shown out in a more recent work on wear of ceramics [21]. A smaller dependence on the material hardness, too, has however been shown in this work (equation 3.3, [21]).

$$V = Const.\ P^{7/6}.H^{-1/2}.{K_c}^{-2/3} \tag{3.3}$$

It is interesting to note that the term L/H in equations 3.1–3.3, above, represents the real area of contact A_r [46]. Hence, contact geometry is expected to play an important part in determining wear behaviour. This issue is considered next.

Contact Geometry

In a recent work [53], it has been shown that wear rate and wear mode show a change with attack angle and contact pressure. This has special significance in view of the fact that varying contact geometries are used in different tests. In general, three types of sliding contacts are employed in laboratory wear tests — point contacts (such as a sphere on a plane) [48, 51], line contacts (such as a cylinder on flat) [49, 50], and conforming contacts (such as a flat on a flat) [51]. Each of these processes has advantages and disadvantages [42]. For example, though point-contact geometry eliminates alignment problems and allows wear to be studied from the start of the test, changing surface temperature and stress levels, with the progression of wear, require more complex data analysis and comparison techniques. Moreover, the stress differences affect wear performance studies in cases where wear mechanisms are stress-dependent. In conforming contact geometry, generally, "wear-in" is allowed to establish uniform and stable contact geometry. This allows for constant load and stress conditions to exist before taking data, but wear-in phenomena, of much importance for certain applications, especially where wear is small, cannot be observed. The stress dependency, in the case of line contact geometry, lies between that for the point and conforming contact geometries.

Temperature

When contacting solids slide, almost all the work done against friction appears as heat, which is partitioned between the two solids. Two temperatures are of interest: the "bulk" or average temperature, T_b, of the near-contact region, and the "flash" or local temperature peaks, T_f, at the asperities on the surface where true contact is actually made. The local increase in temperature influences the rate of wear and (together with the other variables of equation 3.4) determines whether severe wear, or heat induced mechanisms, involving oxidation, chemical reaction or thermal softening and shock , will dominate [39].

$$W = f(F/A_n, v, ThermalProps., Mat.Props., Geometry) \tag{3.4}$$

In the above equation, F/A_n is the load F carried by the nominal contact area A_n and v is the sliding velocity.

3.5.2 Operating Conditions

The operating conditions, just as any other test variable, are dictated by the individual testing program of each group. However, certain conditions like humidity are not always easy to regulate [48]. Similarly, the sliding and loading conditions are test dependent. Though most investigators refer to high and low stress levels, infact very few quote numbers. It so appears that these conditions are relative and depend on other factors such as contact geometry. Hence, a load which might be low in a certain condition can be considered high in another. In the case of sliding velocities, however, it appears that any sliding velocities below 0.1m/s are considered low and those above 1m/s are considered high [39, 55].

3.6 Quantification

Wear quantification is carried out by using several common wear measures, depending upon the testing constraints, such as specimen shape and size, and the quantification method available [42]. Mass or weight loss as a measure of wear [20, 49, 50, 55, 56, 57] is generally suitable if the material densities are the same and when displacement wear and transfer do not occur [42, 56]. Volume loss or displacement [18, 35, 49, 51], on the other hand, though directly attributable to wear, is frequently difficult to measure. Hence in some cases scar width or depth or other geometrical measures [27, 33, 42] and indirect measures, such as the time required to wear through a coating or the load required to cause severe wear or a change in surface reflectance [42] are used, with their inherent advantages and disadvantages.

3.6.1 Cleaning

For all the quantification processes, very intensive cleaning procedures are recommended [18, 20, 31, 35, 49, 56, 57]. The cleaning and drying procedure outlined in one of the works appears to be the most exhaustive [57]. A part of this work is quoted here: "Before testing, specimens were carefully degreased in gasoline–absolute ethyl alcohol(1:1), subsequently in acetone–absolute ethyl alcohol(2:1), ultrsonically cleaned in acetone–absolute ethyl alcohol and dried in hot air. After testing, the specimens were ultrsonically cleaned to remove any debris which was loosely attached to the surfaces. Before and after the tests, specimens were weighed using a precision balance of sensitivity 0.01 mg."

3.7 Qualitative Analysis

•

Once the quantification process is complete, the relationship between wear rate and the different wear processes requires microscopic observation, and evaluation of the effect of the material and operating parameters. For example, a careful examination of wear scar and wear debris, can provide very useful information concerning the wear process [52]. Moreover, since it has been claimed [46] that the major tribological effects are governed by the surface and bulk properties of the contacting materials, a careful measurement of these two kinds of parameters is very important.

For any successful property evaluation, specimen preparation is of primary importance. In a recent work [60] on coating analysis, such specimen preparation techniques have been discussed. Once this step has been completed, any of the numerous available evaluation techniques may be used for examining metallic as well as thermally sprayed materials. Optical [45, 48] or Scanning Electron Microscopy (SEM) [18, 19, 20, 23, 24, 31, 34, 35, 48, 55, 57] may be used for surface and cross-sectional observation. Other techniques for the evaluation of following material properties: hardness [61], fracture toughness [62], cohesion/adhesive strength in the case of coatings [63], surface porosity [64, 65], roughness [61] and deposit thickness [61] may also be applied, depending upon the specific testing requirements of a research group. Furthermore, Raman, infra-red, or Auger electron spectroscopy [65], along with x-ray diffractometry and transmission electron microscopy [24, 66, 67], may be used to identify the crystal structure, and composition of the material and any surface films forming due to the wear tests. The qualitative determination of surface films can help explain wear phenomena in the case of lubricated and high temperature wear.

Among the above listed qualitative evaluation techniques used to study wear and/or thermally sprayed coatings, SEM appears to be the most popular. This can be attributed to the relationship between surface phenomena and wear. Hence, a tribologist has to be able to interpret the results from an SEM examination. Most of this comes by practice and observing the work of other investigators. To facilitate the visualization of some of the most commonly occurring surface phenomena some representative/typical micrographs from the literature are given in Figures 3.11 ([55]).

For instance, the topography of surfaces exhibiting severe wear, as defined by Archard and Hirst [40] is extremely rough and is clearly due to extensive plastic

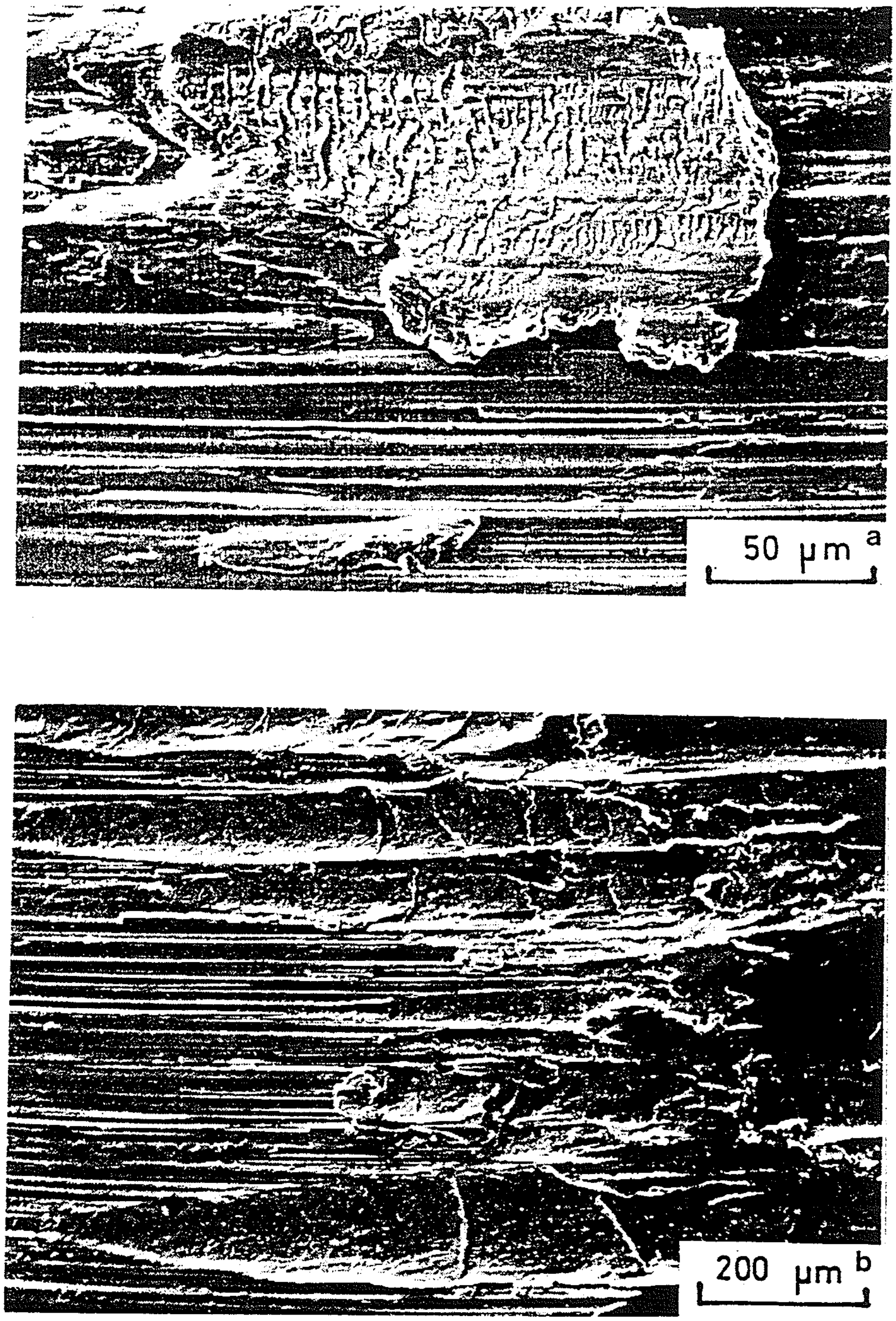

Figure 3.11: Microscopic appearance of surface after a: Abrasive wear, and b: adhesive wear [55]

deformation of the interacting surfaces. On the other hand, the topography of surfaces exhibiting mild wear [40] is extremely smooth (except for the appearance of cracks), thereby indicating the probability that mild wear proceeds by elastic deformation followed by fatigue. Moreover, due to enhanced temperatures at the real areas of contact, oxides are formed (on metal tribo-elements) by reaction with the environment. These then break away at some critical thickness. However, the reaction can be with the lubricant in which the "extreme pressure" additives or, more correctly, "extreme temperature" additives, break down at the real areas of contact of the heavily loaded tribo-elements to form chemical compounds.

3.8 Reporting

After having gone through the earlier sections, it appears that a number of parameters affect wear performance of a material. Thus, it is important to note these factors in order to be able to reproduce the results. A listing of the most important variables that may be recorded is available in the published literature [28, 42, 48, 49, 50, 51]:

a. Apparatus

b. Geometry of contact

c. Type of motion

d. Load

e. Speed

f. Environmental condition

g. Conditions of wearing mediums (hardness, roughness, toughness)

h. Description of materials

i. Description of lubricant and lubrication rate

j. Description of wear-in period, if appropriate

k. Wear quantification technique, and details.

l. Observations of the wear debris amount and morphology, and any protrusions, retained oxide, displaced metal, discoloration, microcracking, or spotting of the materials concerned.

3.9 Epilogue

The subject of wear is very broad. It is not possible to do justice to all the important aspects related to a work like this in a limited work on literature review. Hence, the amount of material presented in this chapter may not cover most areas very extensively. The list of references provided at the end of the thesis, however, is quite extensive. It can provide articles on a wide range of subjects to the interested reader. With this we shall move on to the next chapter.

Chapter 4

EXPERIMENTAL METHODS

The specimen preparation and characterization techniques used in the present work have been listed in this chapter. Moreover, the specimen shapes and sizes, the wear quantification method, the specimen cleaning procedure, and the sequence of wear tests have been presented.

4.1 Specimen Preparation, Shapes and Sizes

The composition of the coated surfaces was determined by the specific objectives, i.e. to evaluate the relative wear performance of the three coatings. There was no limitation on the kind of base material to be used for the specimens prepared for the wear tests. Hence, mild steel was used because of its easy availability. For the bond strength tests, however, cast iron base was preferred, since cylinder liners are made of grey cast iron. The slider material was chosen to be nodular ductile cast iron. Piston rings of this composition are used in actual diesel engine liners.

Different shape and size of specimen and pin/slider were used for the different objectives:

Coated Specimens: Rectangular shape

For test methods and dry tests– length: 48 mm, Width: 12 mm and Height: 6 mm.

For comparative tests– length: 48 mm, Width: 25 mm and Height: 6 mm.

Slider/Pin Specimens:

For test methods and dry tests–Rectangular shape. length: 20 mm, width: 4.85 mm and thickness: 2.55 mm.

For comparative tests–Piston ring of outer radius 12 mm.

Having decided on the above mentioned details, the specimens were sent out for preparation of coated surfaces.

The coated specimens were prepared by using: (i) TAFA metal arc gun and TAFA 60TB wire for AS, (ii) Metco plasma gun and pure $Cr_2 0_3$ powder (METCO 106FP_NS) for PC, and (iii) electrochemical hard chrome process for EC. Manufacturers' specifications required for producing the coatings were followed during the application. The wear test specimens were ground to achieve flat and smooth surfaces. A carborundum wheel rotating at 2300 rpm was used for initial grinding to achieve uniformly thick wear specimens with flat surfaces. For dry tests, the specimens were tested without further surface modifications. For lubricated tests, the specimens were further ground on 120 grit SiC grinding paper.

4.2 Specimen Characterization

The characterization of the test specimens was carried out by means of hardness measurements, surface profilometry and optical and scanning electron microscopy (SEM). In majority of cases, the images taken on the SEM were secondary electron images (SEI). Energy Dispersive X-Ray Analysis (EDX) was also performed, where necessary, on the SEM. Hardness measurements were conducted on the specimen cross-sections and surfaces using a Leitz microhardness tester with a load of 300 gm. Surface profilometry was performed on the polished surfaces before wear testing to obtain the roughness of the deposited coating. The microstructural analysis of the coating was performed using a Nikon inverted optical microscope and a JEOL JXA-840 Scanning Electron Microanalyzer (SEM). The Cr_20_3 coated specimens had to be sputtered with a very thin conductive film of gold for SEM observations.

4.3 Adhesion/Cohesive Strength Tests

The adhesion/cohesive strength tests were conducted to determine the bond strength of the AS and PC coatings sprayed on ductile cast iron coupons (25.4 mm in diameter and 50.8 mm long) as per the ASTM C633-79 standard test method [68]. The surfaces of the loading and substrate fixtures were glued together using an adhesive cured at $170 \pm 5^o C$ for 60 minutes. The surfaces were compressed by means of a support device which maintained axial alignment, and this entire assembly was kept in the oven in order for the adhesive to achieve the maximum cured strength.

The pull-off test was subsequently performed at a rate of 0.001 mm/sec. in an Instron model 1137 tensile testing machine modified according to the testing requirements of the above-stated test method. The load at failure and the type of failure were recorded for each test.

4.4 Wear Tests

The wear tests were performed on a specially fabricated wear test rig. The development of this rig has been discussed, in detail, in the next chapter. In brief, the rig was designed to be able to conduct unlubricated and lubricated, reciprocating, sliding wear, under varying conditions of applied load or contact stress and under conditions of room to high temperature. Of the latter, temperatures up to 200^oC could be achieved by virtue of three elements embedded, just under the specimen, in the specimen holder. Each of these elements produced heat equivalent to 618 Watts. In addition, the specimens could be relocated to the same spot, on the test apparatus after the removal and examination of the specimen and slider/pin, following the completion of a wear test. This was essential for studying the progression of wear with increasing sliding distance. The description of the wear test rig is presented next.

A schematic of the wear test rig and its operating parameters are given in Figure 4.1 and Table 4.1, respectively. The operation of the test rig can be explained using Figure 4.1: The specimen (1) with the coating on its top surface was held in place in a specimen holder (2). The piston ring (3) was held in a piston ring holder (4) which was attached to a slider (5) whose reciprocating motion on two hardened shafts (6) was facilitated by a drive mechanism (7) through a connecting rod (8). The contact between the two surfaces was produced by the application of load (9) which lifted the specimen holder with a parallel arm-linkage mechanism (10). The lubricant drop rate was controlled using a needle valve (11) connected to a lubricant reservoir (12). The temperature of the specimen could also be controlled by a set of heaters embedded into the sample holder plate (13). The main set up of the rig was adjusted at an angle to the horizontal by using adjustable support bars (14) fixed on the frame (15). This provided for the oil to flow down where it was collected in a reservoir (16). In the present work, the specimen was oriented at an angle (10^o) to the horizontal.

Table 4.1: Wear Test Rig Operating Parameters

Cycles per minute	415
Wear track length (mm)	30
Sliding distance per cycle (mm)	2 x 30
Angle to ground	10°
Atmosphere	unregulated laboratory air
Humidity (%)	38 - 40

Depending upon the testing program the loading and lubrication condition were determined:

4.4.1 Test Methods and Dry Tests Objectives

The dry tests involved the unlubricated room temperature wear of a stationary arc-sprayed martensitic stainless steel (AS) coating against a martensitic nodular cast iron (CI) pin in reciprocating, sliding motion. A 10kgf or 98N load was used to force contact between the two surfaces. The shapes and sizes of specimen/pin used for the tests have been described earlier in the chapter. The approach to testing was designed so as to able to study the progression of wear under the conditions described above. This approach was as follows.

The tests were conducted for a certain duration after which the specimen and pin were removed to study the surface characteristics of the specimen in the SEM, visual measurement of pin contact area, and measurement of mass loss of both the specimen and the pin. The pin and specimen were then relocated to their respective positions on the rig and the testing was continued for the next time duration. This process was continued till very loud noise and strong vibrations in the rig indicated

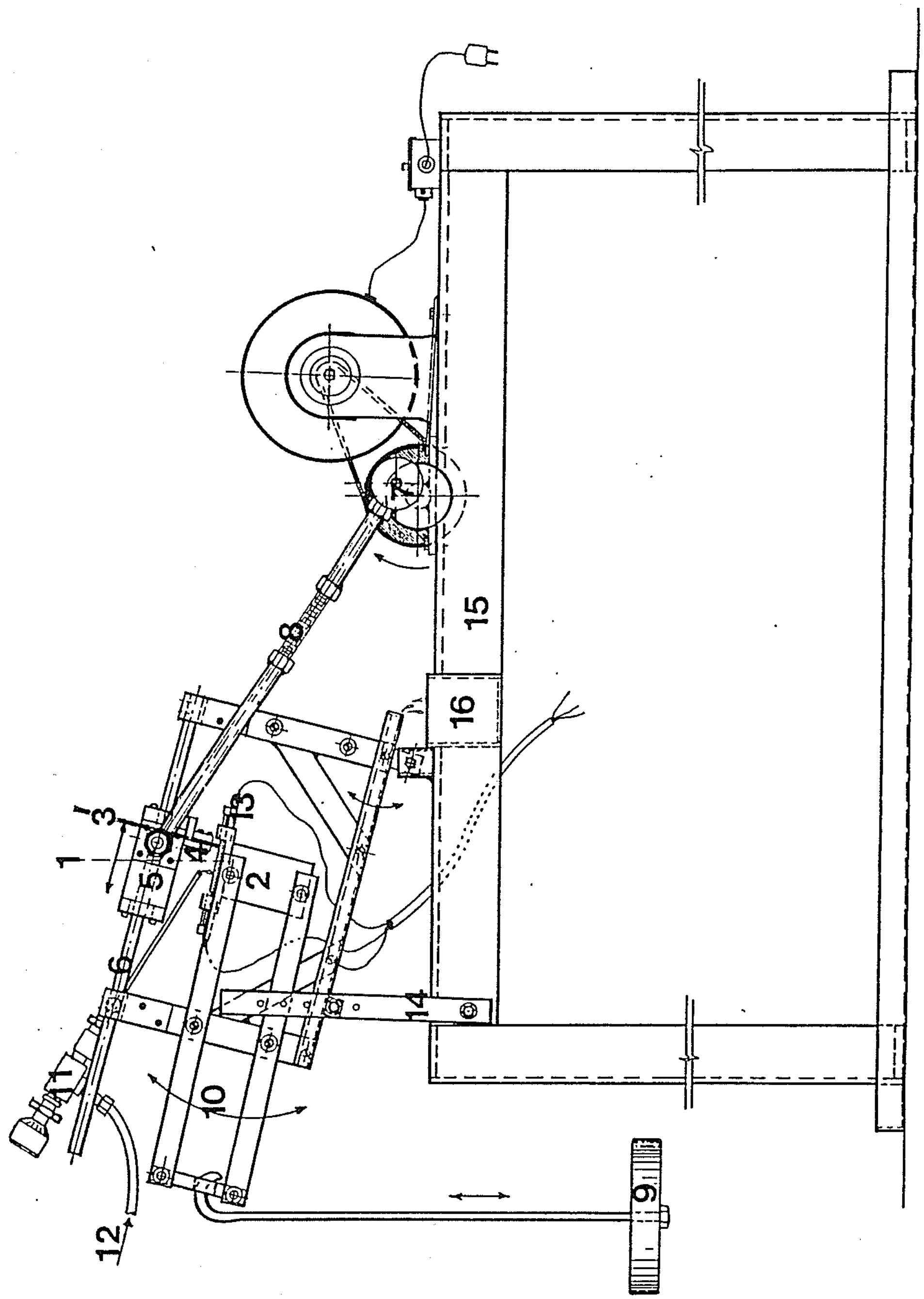

Figure 4.1: Wear Test Rig

the occurrence of scuffing. The testing was terminated at this point for the usual post test observations as described above. Following this, a final four minute test was conducted. As might be clear from the above, only one specimen and one pin were used in one test although many observations of the two were made after various sliding intervals. Three such tests were conducted on three such specimen/pin pairs. These tests/pairs will hereafter be referred to as S1, S2 and S3 and the specimens and pins used for the tests will be referred to as AS1 and CI1, AS2 and CI2, and AS3 and CI3 respectively. The complete sliding conditions and times are given in Table 4.2.

From the above table, it can be noted that in tests S1 and S3 progression of wear was observed for five sliding intervals while in test S2 it was observed for six sliding intervals. Also, it can be noted that in the case of S1 and S3 the fourth sliding intervals were respectively 25 and 55 minutes while in the case of S2 the fourth sliding interval was 20 minutes. This can be explained as follows. In the case of S1 and S3 the testing after the third sliding interval (i.e. after 60 minutes of sliding) was continued till the occurrence of very loud noise and strong vibrations in the rig indicated the occurrence of scuffing. At this point wide-spread wear on pin cross-section indicated that most of the pin cross-section was in contact with the specimen surface and indicated the completion of wear-in period. In the case of S2 however, the testing during the fourth sliding interval was terminated immediately after an indication of noise or small vibrations in the rig. Observations and measurements at this stage could provide insight into the surface phenomena that occur just before the onset of severe scuffing. Following this, the test S2 was continued for a 15 minute interval to reach a stage similar to that attained in the case of the other two tests after four sliding intervals. Testing was stopped in this fifth interval when very loud noise and severe vibrations in the rig indicated the onset of severe scuffing and completion of wear-in. After the completion of these five sliding intervals in test S2 and four sliding intervals in tests S1 and S3, testing was continued for a final four minute sliding

Table 4.2: Sliding Time and Intervals for Test Methods and Dry Tests Objectives

Load used 10kgf or 98N			
Sliding Interval Number	Sliding Time for Each Specimen/Pin Pair (min)		
	S1	S2	S3
1	20	20	20
2	20	20	20
3	20	20	20
4	25	20	55
5	4	15	4
6		4	
Total Time=	89	99	119

interval in all the tests. This was expected to provide insight into the wear processes that occur after wear-in has been completed.

4.4.2 Comparative Tests Objective

For the objective to evaluate the comparative wear performance and to study the wear mechanisms of three coatings at three different load levels under lubricated reciprocating sliding wear, the following test procedure was adopted:

The coating materials used were AS, PC and EC and the sliding material was CI. The specimen shapes and sizes used for these tests have been described earlier. Hereafter, the specimens will be referred to as AS, PC, EC or CI.

The wear tests were run for 8 hours (200 000 cycles) at a lubrication rate of one drop every 4 minutes. Three different load levels were used. Only one test was run on each wear track, after which the specimens were removed for wear quantification

Table 4.3: Operating Parameters for Comparative Tests Objective

Contact load (N)	98, 196, 392
Number of cycles slid	200,000
Lubricant	10W30 at 24°C
Lubrication rate (one drop = 0.02 ml)	1 drop every 240 sec.
Specimen heated to	80°C

by profilometry and by taking the impression of the piston ring wear scar. The test specimens were heated to 80°C. The lubrication oil used was 10W30. These parameters are also listed in Table 4.3.

4.5 Wear Quantification Methods

The wear measurement schemes available were mass measurement, linear dimensions of wear, and area and volumetric measures.

4.5.1 Mass Loss Method

For the test methods and dry tests objectives, mass loss method was used for wear quantification. This method involved the measurement of wear rate for a particular test by taking the difference in mass of the specimens before and after the test. A Mettler H35 weighing system was used in this method. The accuracy of this system was 0.1mg. Since the specimens used in the wear tests were of the order of 30 gram mass for the coated specimens and 2 gram for the pin specimens, the balance was calibrated with 30 and 20 gram standard mass before each weighing session of coated specimens and with a 2 gram standard mass for each pin weighing session. In general the calibration of the balance was excellent. In order to ensure consistent values of the specimens to be weighed an extensive procedure of cleaning, drying and storing, given ahead, was followed.

4.5.2 Volume Loss Method

For the comparative tests objective, volume loss method was used for wear quantification. After wear testing, the trace of the wear track was recorded to calculate wear volume. A surface profile measuring system, Surtronic 3P, was used for this purpose. It was used to plot the cross-sectional area of the wear track formed on the test surface (Figure 4.2a). The mean of the area (equation 4.1)

$$A = A_1 - (A_2 + A_3) \tag{4.1}$$

from three profiles along the scar was then used to calculate the volume loss of the material by taking the product of this area and the length of the groove, which was the length of one forward or backward movement of the slider. This technique of wear quantification is very similar to that used by other researchers [35]. The volume loss of the slider–the piston ring–was determined by taking an impression of the worn surface area on the piston ring. This could be closely approximated to a shape such as that of an ellipse (Figure 4.2b). The loss in the thickness of the piston ring for a wear scar (Figure 4.2c) was used to calculate the appropriate volume loss for a wear spot.

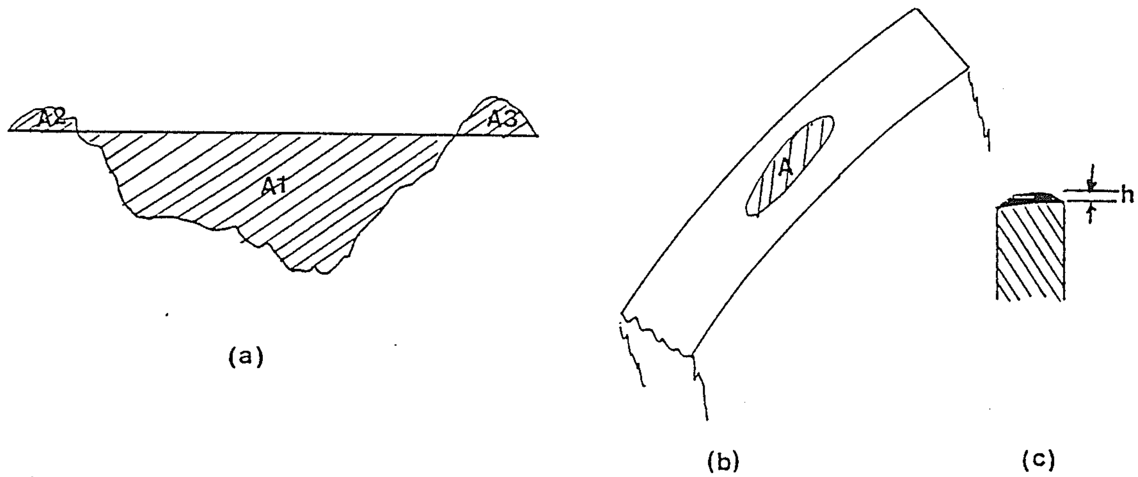

$$A = A_1 - (A_2 + A_3) \qquad\qquad V = f(A, h)$$

Figure 4.2: Volume loss method

The loss in volume could then be converted to mass loss using the appropriate material densities.

4.6 Specimen Preparation Schemes

Before the start of a weighing session the following cleaning procedure was followed. The specimen and pin were first washed in soap to remove any loosely held particles. This was done to avoid any flaking off, of such particles, in subsequent handling and hence a discrepancy in results. After this wash, both the specimen and the pin were ultrasonically cleaned in ethanol for five minutes, to remove loose debris, and were cleaned with a cotton ball to wipe such debris. They were finally ultrasonically cleaned in acetone for five more minutes to remove any remaining debris and/or any undissolved greases/oils. This procedure was expected to remove most of the removable debris. After this, the specimens were carefully removed with the help of pliers and were cleaned of any debris clinging to the surface by squirting it with acetone. The specimens were then air dried, first by a blow drier and then in an air blown furnace, at 100^{o}C for 10 minutes. This was done to flush and dry any cleaning fluids trapped inside the porous surface of the coated specimens. Immediately after this step, the specimens were put in a dessiccator, and put under vacuum for two hours, to let the specimens cool down to the temperature in the balance room. This procedure was expected to prevent any oxides or water vapors from adhering to the specimens. Overall, the procedure adopted was fairly exhaustive and should minimize any variations in actual experimental measurements reported in the literature [18, 20, 31, 35, 49, 56, 57].

Chapter 5

RESULTS AND DISCUSSION

The contents of this chapter include results from the material characterization, bond-strength tests and wear related work. As part of the latter, the development of the wear testing apparatus and wear quantification schemes have been discussed. Moreover, the reproducibility of the wear tests, the progression of wear in AS and the results from the comparative wear tests have been presented and discussed.

5.1 Material Characterization

The cross-sectional microstructures of the coatings are shown in Figure 5.1. Figures 5.1a and 5.1c are optical micrographs of AS and EC respectively, while figure 5.1b is a SEM secondary electron image (SEI) of PC. In figures 5.1a and 5.1b the formation of a splat like structure, typical of thermally sprayed coatings, can be noted. Such a microstructure results from the spreading out and splattering of the molten metal particles, some of them oxidized during their travel from the nozzle of the spray gun to the substrate surface. Voids result as the growing deposit traps air. The build up of such a structure has been recently reviewed in the literature [8].

The electrochemically deposited chromium (hard chrome), on the other hand, has a much more uniform and dense structure [Figure 5.1c]. Some stress cracking typical of hard chrome [3] was noted in the EC coating (Figure 5.2). The micrograph of the piston ring cross-section [Figure 5.1d] reveals that it has a martensitic nodular cast-iron microstructure. The hardness and surface roughness of the three coatings and the cast iron piston ring is given in Table 5.1. It can be seen that the hard chrome had the smoothest surface which could be attributed to the dense nature of the electroplated chromium. On the other hand, thermally sprayed AS and PC coatings contained porosity which contributed to the surface roughness. With respect to material hardness, EC was the hardest followed by PC, CI and AS in that order.

5.2 Adhesion/Cohesive Strength Tests

The bond strength test data are given in Table 5.2 which clearly indicate that the failure in both the coatings was the cohesive type. The strength at cohesive failure for the steel (AS) is about half that of the values reported by another group of investigators [12] for a similar coating. Although the failure type reported in both the investigations is cohesive, the discrepancy between the two bond strength results could be attributed to a possible variation in coating process parameters. As regards the Cr_20_3 (PC), a similar work [18] reported adhesive failure at 2.84 MPa on the enamel/substrate interface in a multi-layered Cr_2O_3 coating. The cohesive strength of Cr_2O_3 under tension can thus be qualitatively assessed to be greater than 2.84 MPa. In the present work, a noteworthy reproducibility of the results and comparison with already published results [12, 18] provides confidence in the quantitative estimation of bond strength. Moreover, it can be safely concluded from these results that the adhesion of the two coatings to the cast iron base is stronger than their respective cohesive strength values.

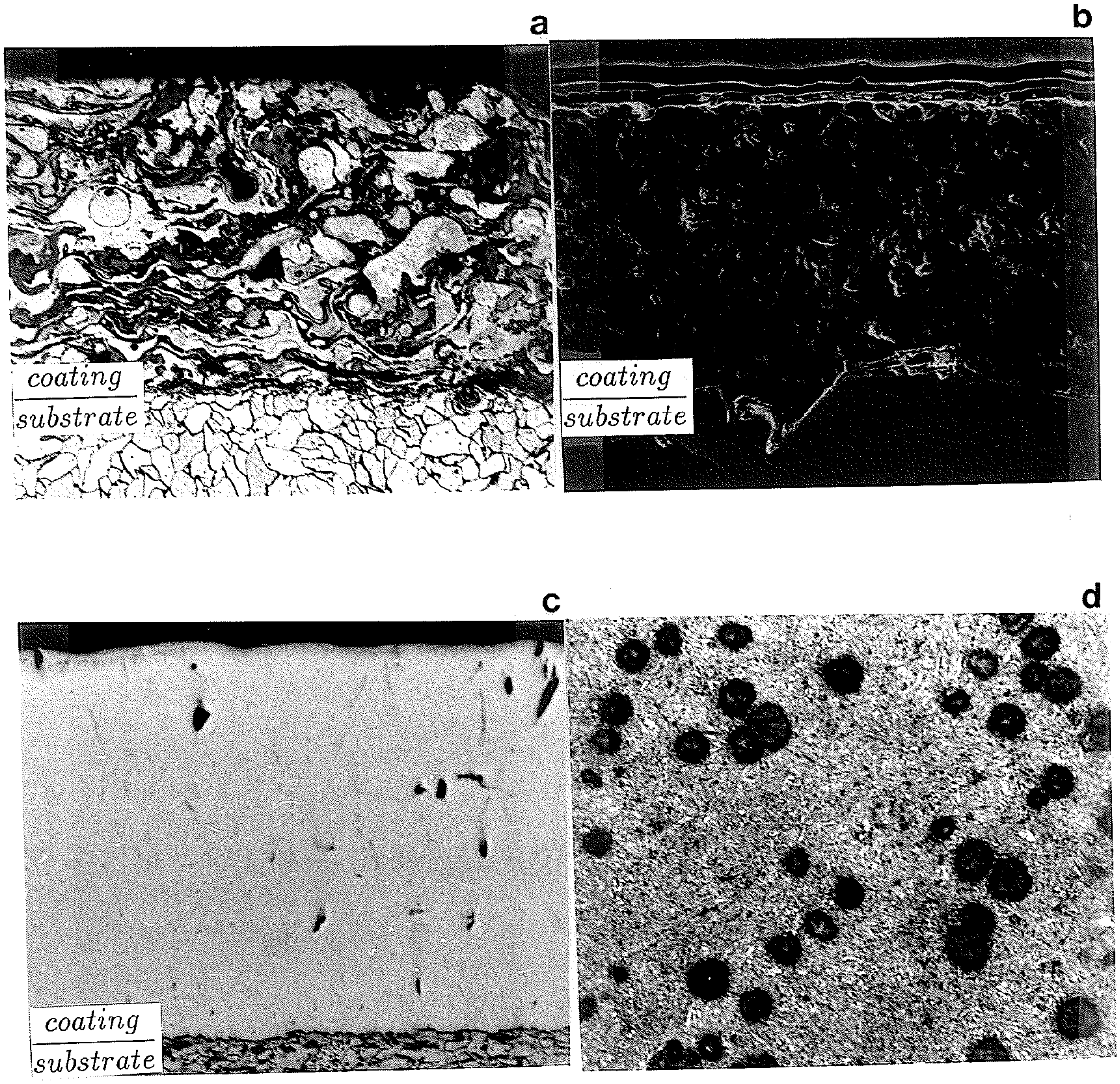

Figure 5.1: (a,c,d): Optical micrograph of AS, EC and CI cross-sections, respectively (200X); (b): SEI of PC cross-section (450X)

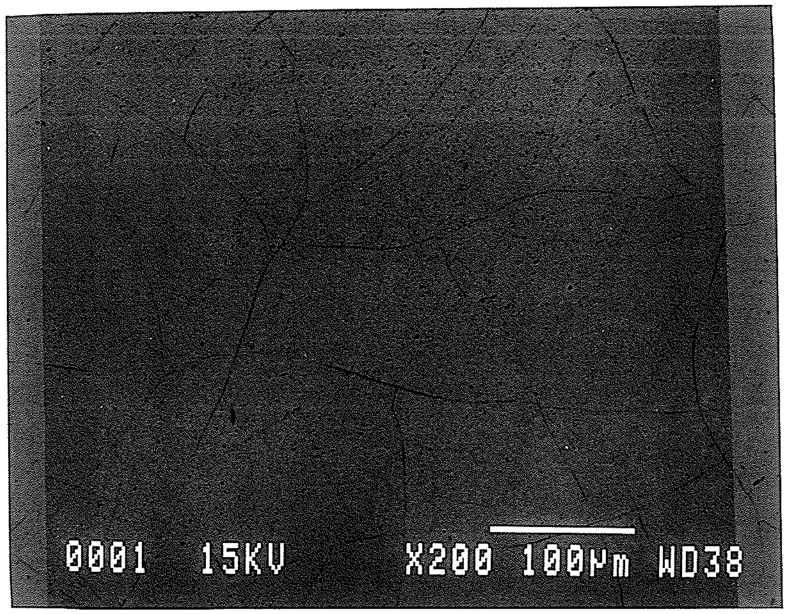

Figure 5.2: Network of cracks on ground and polished EC surface

Table 5.1: Cross-sectional Hardness and Surface Roughness Values

Identification letters	Material	Hardness (DPH_{300})	Roughness (R_a,μ)
CI	Piston Ring	427	1.80
AS	Arc-sprayed Martensitic Stainless Steel	262	0.36
PC	Plasma-sprayed Cr_2O_3	533	0.33
EC	Electrochemically deposited (hard) chromium	927	0.10

Table 5.2: Adhesion/Cohesive Strength Test Results

Specimen	Surface Roughness (R_a,μ)	Stress at Failure (MPa)	Mode of Failure
PC			
1	4.3	6.92	Cohesive
2	4.5	1.79	Cohesive
3	4.0	6.82	Cohesive/Adhesive*
4	4.5	4.39	Cohesive
5	4.6	3.55	Cohesive
Average	4.4	4.69	
AS			
1	15.0	5.72	Adhesive
2	14.5	16.08	Cohesive
3	16.0	15.45	Cohesive
4	16.2	17.50	Cohesive
5	14.7	6.59	Adhesive
Average	15.3	12.26	

*: Failure at both the adhesive and inside the coating

5.3 Development of Wear Test Apparatus

5.3.1 The Objective

The objective was to develop a wear testing apparatus which could simulate the conditions in a diesel engine liner. Thus, it was decided to build an apparatus which could be used for conducting high temperature, lubricated, reciprocating sliding wear under varying conditions of applied load or pressure. An added feature could be varying the speeds of sliding. Also, it was thought necessary to be able to relocate the specimens in case the progression of sliding wear with sliding distance needs to be evaluated. With this in mind, the design of the wear testing apparatus was attempted.

5.3.2 Specimen and Slider/Pin Shapes and Sizes

The main design consideration was the availability, shape and size of the coated specimen and the mating material. It was desired that the slider should have a small contact with the coating. This would permit the use of smaller size specimens. Moreover, a smaller slider contact area meant higher contact stresses and hence faster wear rate and data collection. The specimen size was basically dependent on the simplicity of testing and the possibility of using either of the two available wear quantification schemes. In unlubricated tests, since mass loss was substantial, the mass loss method was used. In lubricated tests, however, the wear of the specimens was too small to be accurately recorded on the balance used. Hence, volume loss method, using the profilometer, was applied. In such a situation, as long as the profilometer can scan the entire width of a wear scar, large size specimens can be used. Having determined such a basis, the optimum size of the specimen and pin/slider was determined.

The specimen

For the coated specimen, a rectangular shape was preferred. Such a shape is easily coated (the coated specimens were provided gratis by the organizations listed in the previous chapter) , tested, and analyzed. Since, 6mm thick material is the most conveniently available, is sufficiently thick to be able to withstand the high temperatures from thermal spraying, and could be used without adding substantial weight to the specimen, the thickness of the specimens was kept at 6mm. To conveniently observe the worn surfaces, of a specimen about 6mm thick, in the scanning electron microscope the width was limited to about 25mm. The specimen could be about 50 mm long and still fit in the apparatus. For the test methods and the dry tests objectives, however, the width, being the only flexible dimension, was reduced to 12mm. The width of the specimens also permitted multiple tests (on different wear tracks) on each specimen. Hence, SEM observation of worn surfaces from many tests was simultaneously possible.

"Slider" or"Pin"

The determination of slider shape was, however, dependent on individual objectives of the study. For the case of the test methods and the dry tests objectives–the reproducibility of the test apparatus and the wear mechanism study–the shape of contact is not important [28]. Hence, for this part of the research, the shape of the slider was chosen to be a cuboid called a "pin". Such a shape, as explained earlier [42], is easier to work with. In the case of the comparative tests objective, the use of an actual piston ring shape was desired. This selection was based in realization of the fact that in a diesel engine cylinder, a small metal-to-metal contact area gradually increases to give catastrophic wear (in cases where it is caused) [45]. The wear progression is in the order of wear-in, abrasion and corrosion, and adhesive wear. Hence, small arc sections from the piston ring were used as slider sections. It was, however, found that the orientation and angle of contact of the different slider sections, from different trial test runs, varied very widely. Since this was unacceptable, a new arrangement to hold the slider was attempted. In this arrangement, a groove was so machined in an aluminum block that the entire piston ring could fit in it. The groove was as deep as the thickness of the piston ring and was cut in the shape of an arc of radius equal to that of the piston ring. An aluminum plate, secured on to the block by three screws could hold the piston ring in place between the block and the plate. Once a test on a spot on the ring was completed, the ring was rotated to another spot by releasing and re-screwing the aluminum plate. This allowed for similarity in the shape of contact, because the piston ring was always at the same orientation/angle to the wear surface in all the wear tests. Moreover, since the use of the mass loss method was ruled out, for the comparative tests objective, the use of the entire piston ring was not inhibited.

5.3.3 Sliding Direction and Relocation

The sliding direction, for the slider or pin, was decided to be reciprocating, along the length of the 50mm x 25mm or the 50mm x 12mm face of the specimen. The specimen could be tightened in place and pressed against one edge of the platform, which held the specimen, by a set of screws. The specimen side on the back of the sliding face would rest on the platform. The other two sides of the specimen could be used to relocate it to the same spot after each session of an increasing cycle test. The increasing cycle test was designed for the dry tests objective, to study the progression of wear with increasing sliding distance.

5.3.4 Stroke Length

Once the specimen length was fixed, the stroke length was essentially determined. It was 30 mms, allowing for the top part of the specimen (about 20 mms) to be used for the drop of oil to fall.

5.3.5 Sliding Speed

It has been stated earlier that a high sliding speed causes high flash temperatures and hence severe wear. Since in this testing program, the objective was to study wear as it normally progresses in a diesel engine cylinder, a low sliding speed was preferred. Keeping this in mind, a DC motor with an rpm of 1725 was selected. The number of cycles per minute (415) and hence the sliding speed of 415 mm per second (the slider moves 30 mms in each of the two strokes in a cycle) was determined by the ratio of available pulleys for down-stepping the revolutions. It must be clarified, however, that the sliding speed stated above was the maximum possible during a stroke. At the end of a stroke, the instantaneous velocity is known to be zero.

5.3.6 Specifications of the Motor

As can be noted from the last sub-section, the specifications of the motor (to drive the pulley and shaft mechanism) were determined by the testing requirements. A DC motor with a Horse Power of 0.25, giving an rpm of 1725 was thought to be adequate to slide the slider, since very small friction forces were expected for the loading program.

5.3.7 Loading Program

The loading program of 10, 20 and 40 kgf was selected because it gives a variation from medium to heavy loading. It was later found that even 10kgf load was heavy for unlubricated tests with the specimen and pin.

5.3.8 Lubrication rate

The objective was to provide boundary lubrication and therefore lubrication rates were kept small, about 0.04 ml every four minutes. Similar lubrication rates, for simulating diesel engine wear, have been reported in the literature [45].

5.3.9 The Environment

The environment was laboratory air. The humidity in the room (38-40%) was constant throughout the study. The temperature in the room was $20 - 22^{o}C$.

5.3.10 The Operating Temperatures

For the test methods and dry tests objectives, room temperature tests were desired. For the comparative tests objective, however, the platform holding the specimen was heated to 80°C. This was done in realization of the effect of lubricants in reducing metal-to-metal contact and hence in reducing the bulk and flash temperatures. Hence, it was thought appropriate to have at least one specimen at a higher temperature close to actual operating conditions in the cylinder liner. The idea was that the temperature could contribute to the effects of high friction and operating temperatures inside a cylinder liner which reduce the lubricant thickness, decrease its viscosity, and cause higher flash temperatures all of which lead to oxidative wear of cylinder wall sections.

A very high temperature was not desired because it would have caused a predominance of oxidative wear, led to a larger requirement on lubricant rate, and created hazardous working conditions.

5.3.11 Debris Collection

Since debris collection and analysis is one of the trends in recent research works on wear mechanism studies, it was thought appropriate to be able to collect the wear debris. The reciprocating motion of the slider was expected to help in debris collection because of the rejection of the debris by forces acting in either direction of slider motion. Moreover, the collection of debris at the end of the coating, carried there with the lubricant flow, along and down the coating, was also expected.

5.3.12 Inclination

Most wear testing apparatii have specimens oriented horizontally [2, 18, 31, 35, 45, 48, 65]. In some cases the specimens are oriented vertically [19]. Both orientations have advantages and disadvantages. Hence, in this work a combination of the two orientation schemes was attempted so that features from both could be incorporated. It was thought that the debris, while flowing down, would cause conditions similar to third body contact, but since it was expected to ultimately be removed from between the mating surfaces it would not cause a pseudo layer of debris which would prevent metal-to-metal contact, the function normally performed by oxide layers or the lubricant. This feature in the testing apparatii has not been reported by other investigators.

5.3.13 Stiffness of the Rig

The stiffness of the rig, discussed elsewhere [52], was dependent on the machining operation and the material used. During machining, attempts were made to allow only close tolerances in the dimensions of parts. Hence, the stiffness of the apparatus was assumed to be good. No macroscopic observations to the contrary were made, although microscopic deflections could not be ruled out.

5.4 Construction of the Test "Rig"

Once the considerations listed in the previous section, had been taken into account, the wear test apparatus (as shown in Figure 4.1), hereafter referred to as the "rig", was designed and fabricated in the Machine Shop in the Department of Mechanical and Industrial Engineering at the University of Manitoba. Following this, preliminary tests were conducted to evaluate the opeartion of the rig.

5.4.1 Performance Report on the Apparatus

A number of preliminary tests were run on the machine, with the specimen-pin and specimen-ring configuration. In the former tests, it was in general noted that initially the contact between the pin and the specimen surfaces was non-conformal. The apparent contact area grew with increasing wear after which loud noise started to emanate, which subsequently grew louder with simultaneous introduction of vibrations in the rig. The tests were in general stopped at this point. The sliding time taken to reach this stage varied from 10 to 120 minutes. This was taken into consideration for the development of a formal testing scheme. In the case of lubricated tests, no such problem was noted though it was found that weight loss was very small and hence it was necessary to resort to the volume loss method. Following the preliminary tests, a formal wear testing scheme was devised for the dry tests and comparative tests objectives . These schemes have been given in the previous chapter.

5.5 Wear Quantification Methods

In lubricated wear tests, the loss of material even after long testing hours was not sufficient to be accurately recorded in a balance of 0.1 mg precision. Moreover, since it was not possible to weigh the piston ring because of its size, it was decided to use the volumetric measure of wear. The method of measuring wear by linear dimensions was not employed due to certain inherent flaws in this scheme. These have already been pointed out in the previous chapter. For the unlubricated tests, however, since the mass loss was substantial, it was decided to use the mass loss quantification method.

5.6 Results of Wear Tests

Having fabricated the machine, conducted a few preliminary tests and decided on a wear testing and quantification approach, the desired experiments were conducted. The results obtained from these experiments are presented in the following.

The results have been broken into two broad sections. In the first section, results and their interpretation from tests run for the test methods and dry tests objectives have been presented. With regard to the test methods objective, the reproducibility of the wear tests has been discussed. In the second section, the results and their interpretation from tests run for the comparative tests objective have been presented.

5.6.1 Test Methods and Dry Tests Objectives

These objectives involve the unlubricated ("dry") tests on AS under reciprocating, sliding wear conditions. The mating material was a martensitic nodular cast iron pin. The data collection during these tests included the following variables:

1. Time of sliding (min) [t]
2. Applied load (kgf) [L]
3. Apparent contact area (of pin) (mm^2) [A_c]
4. Nominal contact area (of pin) (mm^2) [A_n]
5. Mass loss (of coated specimen) (mg) [M_s]
6. Mass loss (of pin) (mg) [M_p]

Using the above, the following quantities were calculated:

a. Fraction of the nominal contact area (of pin) (A_c/A_n) [f]
b. Sum of specimen and pin mass loss for each test (M_s+M_p) [M_T]
c. M_s/f, M_p/f, M_T/f
d. M_s/t, M_p/t, M_T/t
e. M_s/ft, M_p/ft, M_T/ft

The quantity in 3, the apparent contact area of pin, was found to be increasing with sliding time till at the end of fourth interval in tests S1 and S3 and the end of fifth interval in test S2 it was equal to the nominal contact area of the pin. The values listed in (f) above were calculated by dividing the values in (3) above by the total cross-sectional area of the face of the pin in contact with the wear surface. These are given in appendix B.

The values in 6, d, e and f, above, were plotted against the values in 1, above. Hence, four different types of y-axes and one type of x-axis were available giving four types of x and y axes combinations. For each of these four axes combinations three different graphs (specimen wear, pin wear and sum of the two) were possible. Moreover, each graph had three plots due to the data from three tests (S1, S2 and S3). The three graphs for each axis combination were grouped together on one page. Thus, overall 12 graphs were constructed on four pages representing the data from three tests. The large number of data combinations, required for these were produced by using a computer program which is given in appendix A. The various data files so constructed are given in appendix C. The results from these can be seen in figures 5.3–5.6. The x-axis in all the graphs represents sliding time (t). The y-axis is M, M/f, M/t, and M/ft in Figures 5.3, 5.4, 5.5, and 5.6, respectively. The graph at the top on each page represents the specimen wear, the middle represents pin wear, and the bottom represents the sum of specimen and pin wear. From these figures, the following information can be gathered.

Wear, in the present study as represented by the y-axis values on the 12 graphs, shows two distinct features. One, the initial wear is much smaller than the wear occurring in the final four minute sliding interval. Two, the high wear in the final four minute sliding interval occurs at the point where wear-in of the test surfaces has been completed and the apparent area of contact between them is much larger than in the previous sliding intervals. In the case of test S2 a rising trend in wear can be noticed after the fourth sliding interval. In all the specimens the rise in wear was found to be coupled with a 10 to 20°C rise in specimen bulk temperatures.

The use of various values to represent the y-axis indicates some interesting features. The use of mass loss per unit sliding time as opposed to the use of only mass loss as y-axis reduces the difference between the plots for the three tests. On the other hand, the use of mass loss per unit fractional contact area as opposed to the use of only mass loss as y-axis increases the difference between the plots for the three tests. However, it could not be determined whether the wear depends on contact area

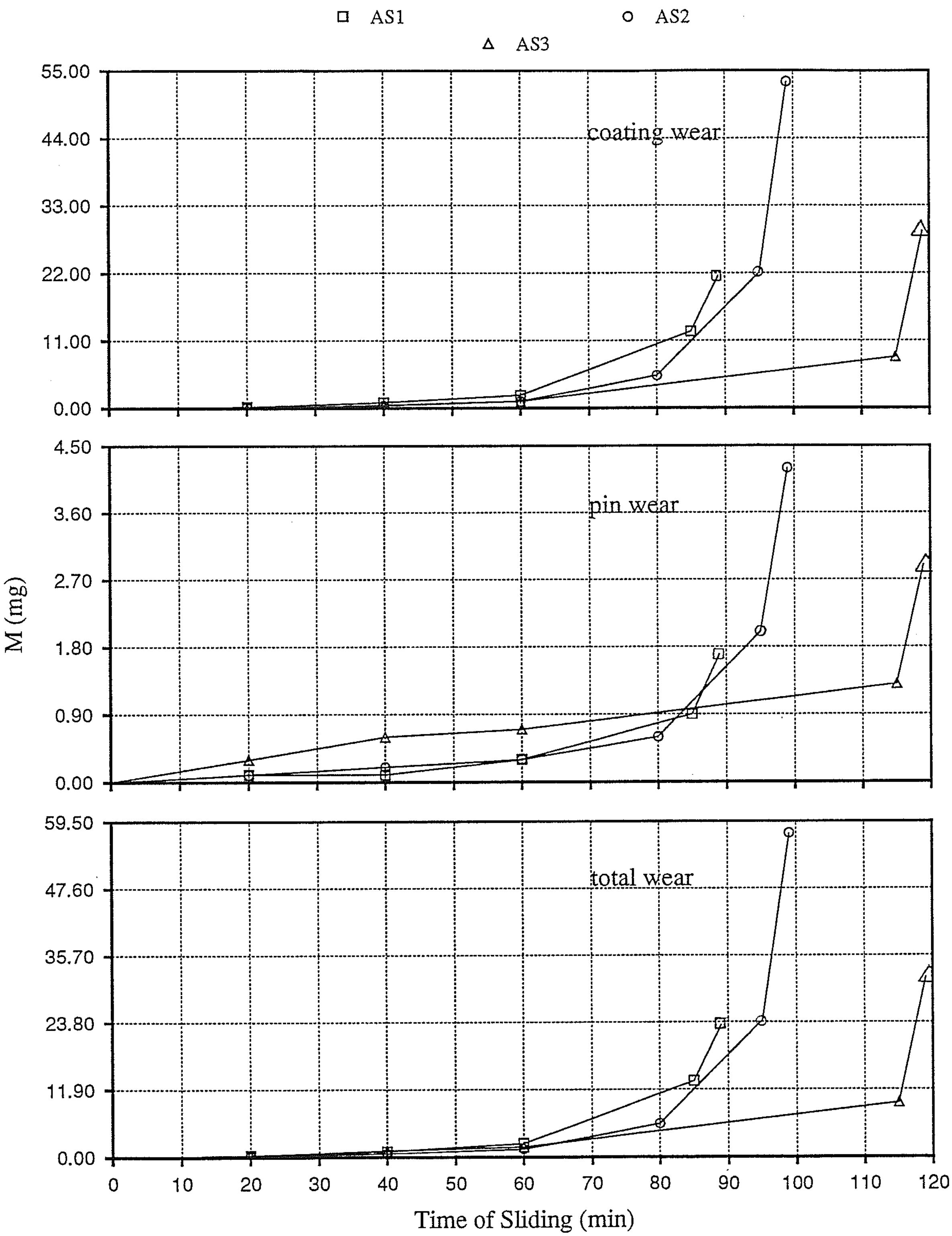

Figure 5.3: Mass loss vs. sliding time of S1, S2 and S3 specimen/pin pairs

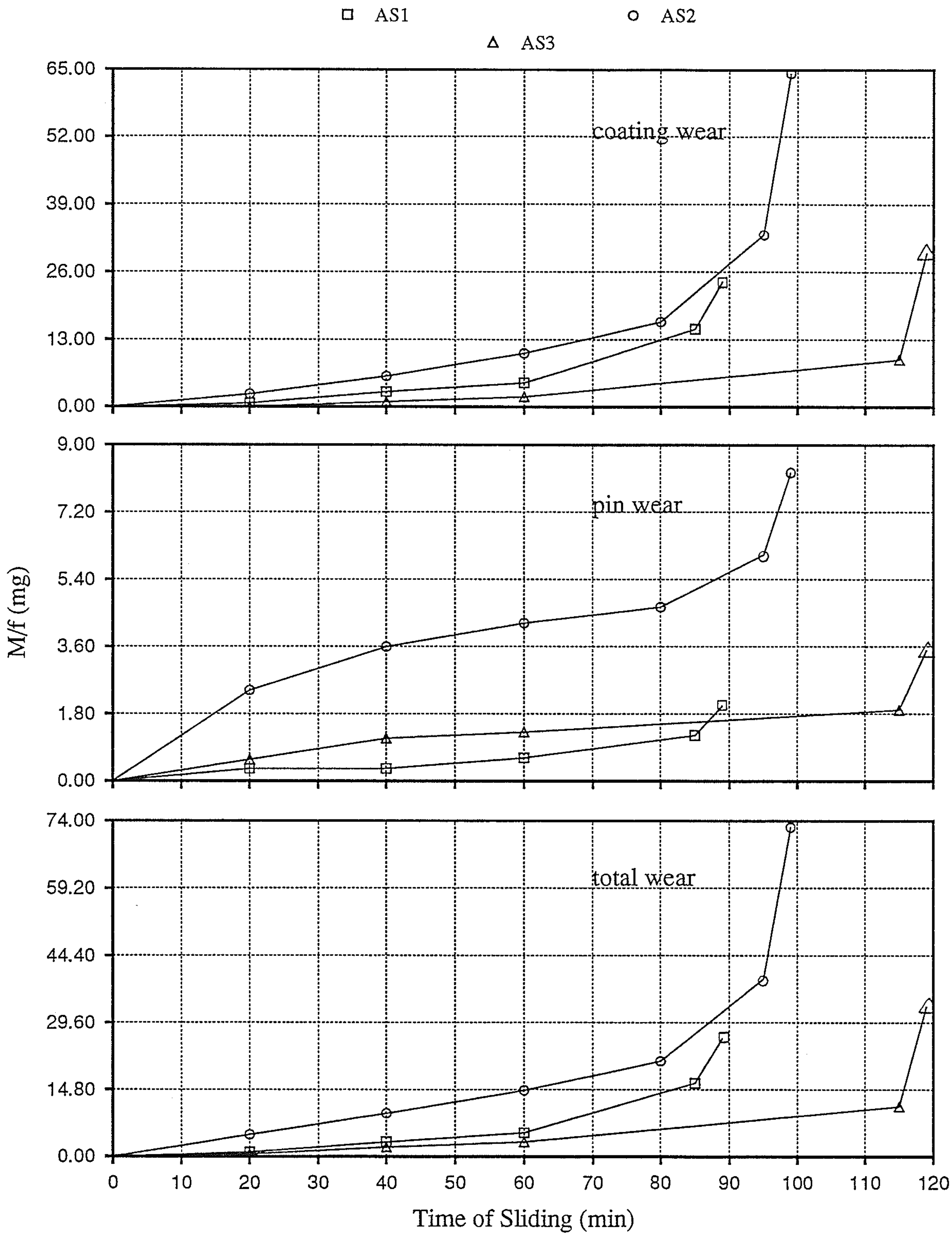

Figure 5.4: Mass loss per unit fraction of nominal contact area vs. sliding time of S1, S2 and S3 specimen/pin pairs

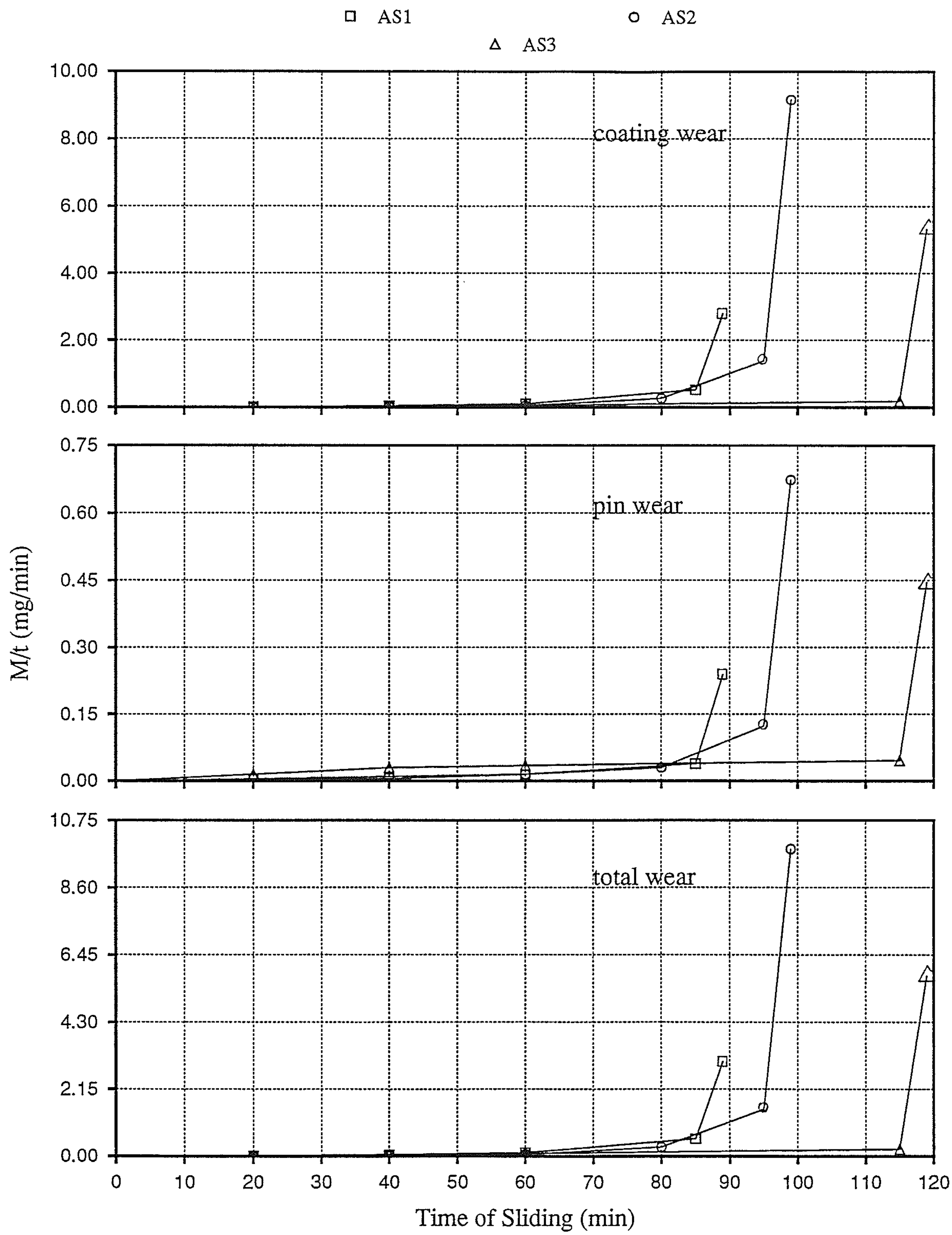

Figure 5.5: Mass loss per unit sliding time vs. sliding time of S1, S2 and S3 specimen/pin pairs

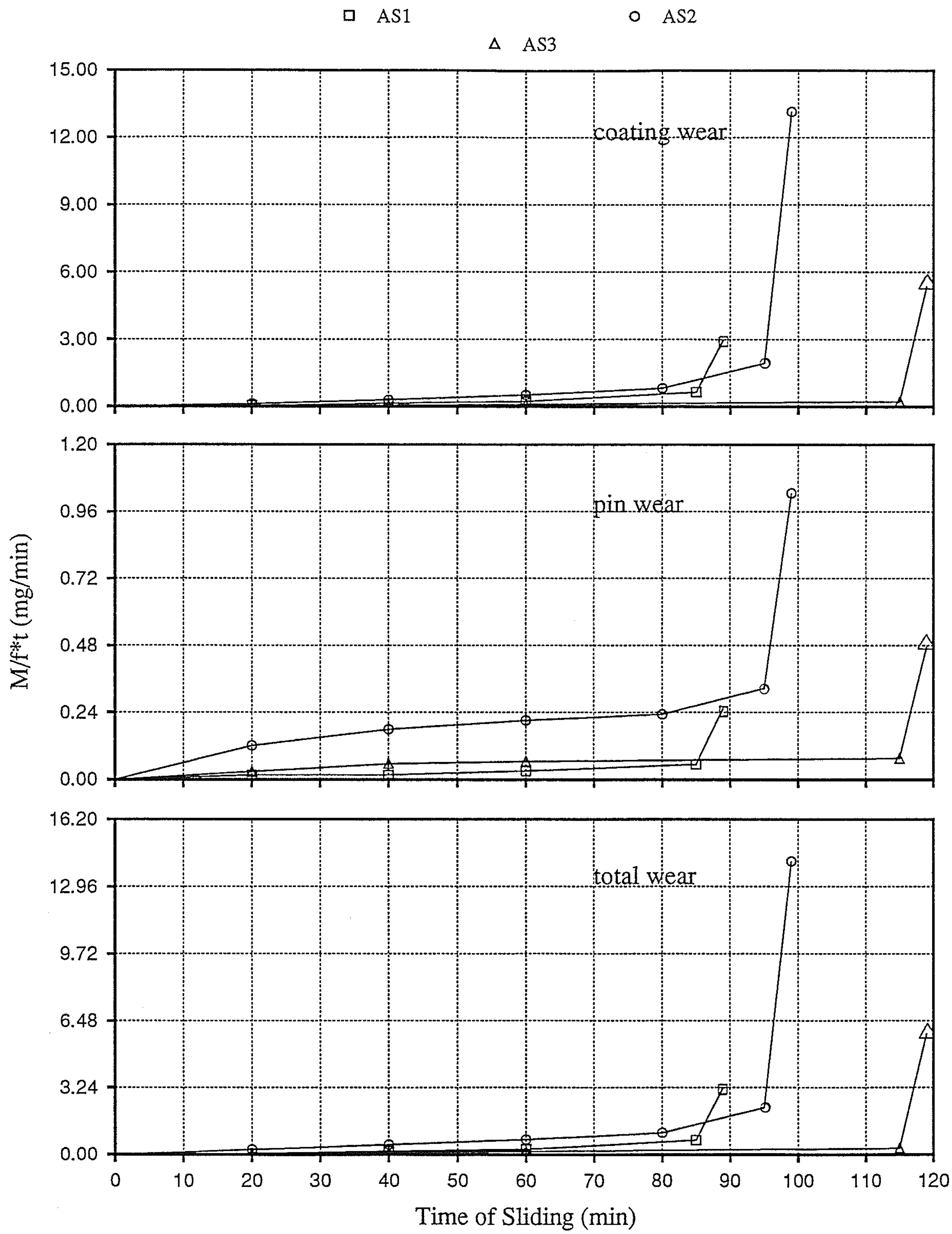

Figure 5.6: Mass loss per unit fraction of nominal contact area and sliding time vs. sliding time of S1, S2 and S3 specimen/pin pairs

or sliding time during either mild or severe wear mechanism. More remarks about the graphs presented above are presented in the following.

The initial low wear corresponds to wear-in period during which gradual wear of the specimen and pin leads to increased contact between the two surfaces. Once this is achieved the wear increases dramatically (the reasons are discussed later in this section). In the case of S2 the rise in wear begins in the fifth interval because the contact area between the surfaces, after the fourth interval, was already so large as to cause minor scuffing. Infact the cause for more wear at the end of fifth interval in the case of S2 than after the fourth intervals in tests S1 and S3 may have been that the fourth interval in the case of S2 was broken up into two. It appears that if test S2 was not stopped at the stage where it was during the fourth sliding interval, then the wear debris and high temperatures that existed at the time of stopping it could have led to observation of severe scuffing shortly afterwards. Then, the increased wear and longer time (15 minute) recorded in test S2 to reach the same stage at which the other two tests were stopped after the fourth sliding intervals would not have been observed. However, stopping the test was part of the experimental plan to study progression of wear during that stage. As a consequence of this, more wear and time was required for the generation of new wear debris that could complete wear-in and generate friction and heat to cause severe scuffing in the fifth interval. This indicates that the rising trend in wear for the fifth sliding interval in test S2 may be a result of imposed experimental conditions. From all of the above it can be noticed that in the present study, wear changes from one of mild type to that of severe type after wear-in of the contacting surfaces has been completed. Similar evidence of changing wear mechanism with increase in contact area and increasing surface damage (wear) with sliding time has been microscopically verified by using the SEM.

The SEM secondary electron image (SEI) of typical AS surface, used for dry wear tests is shown in Figure 5.7. The SEI from wear tests S1, S2 and S3 are given in the following figures. Since there were more sliding intervals during wear test S2 and since it is representative of wear and its progression in the remaining tests, first SEI from AS surfaces in test S2 are presented. Figure 5.8 shows the wear surface of AS2 after the second sliding interval (40 minutes). Figures 5.9, 5.10, 5.11, and 5.12 show the changes in the same wear surface after 60, 80, 95 and 99 minutes of sliding wear, respectively.

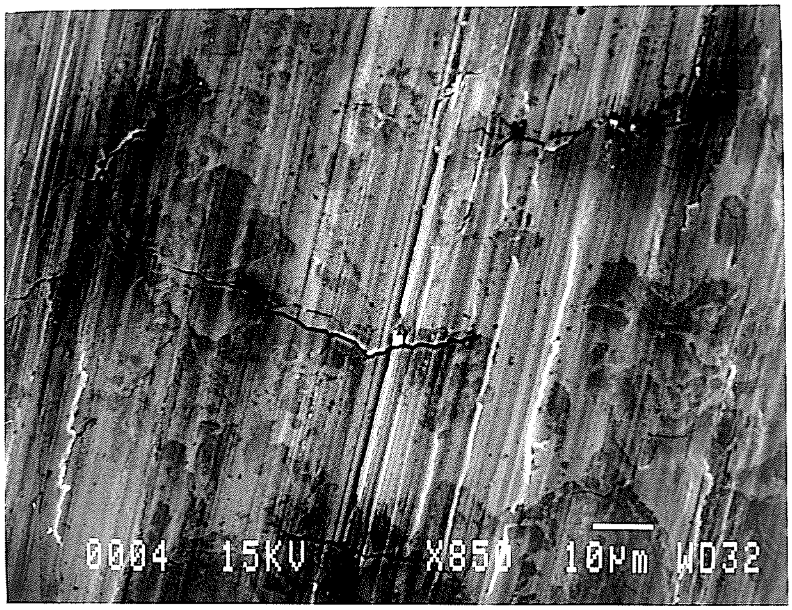

Figure 5.7: Typical as-ground surface of AS, before wear tests

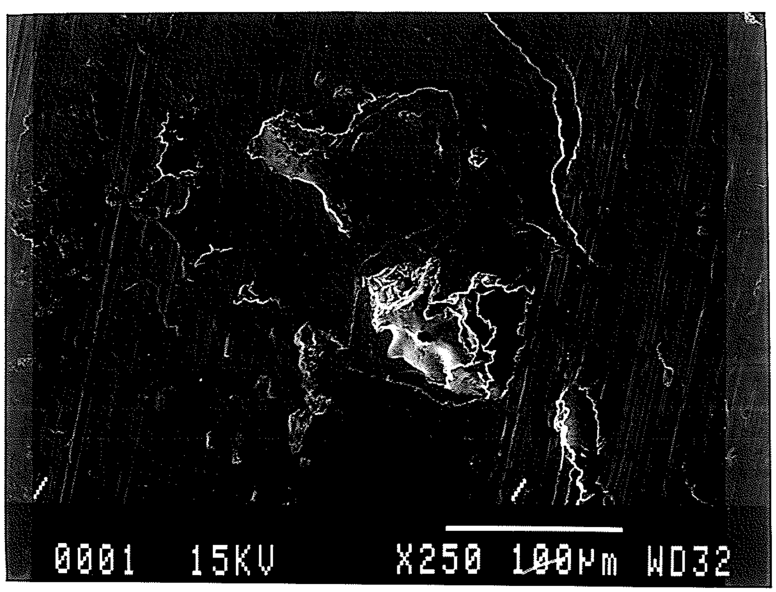

Figure 5.8: Worn surface of S2 after 40 minutes of sliding

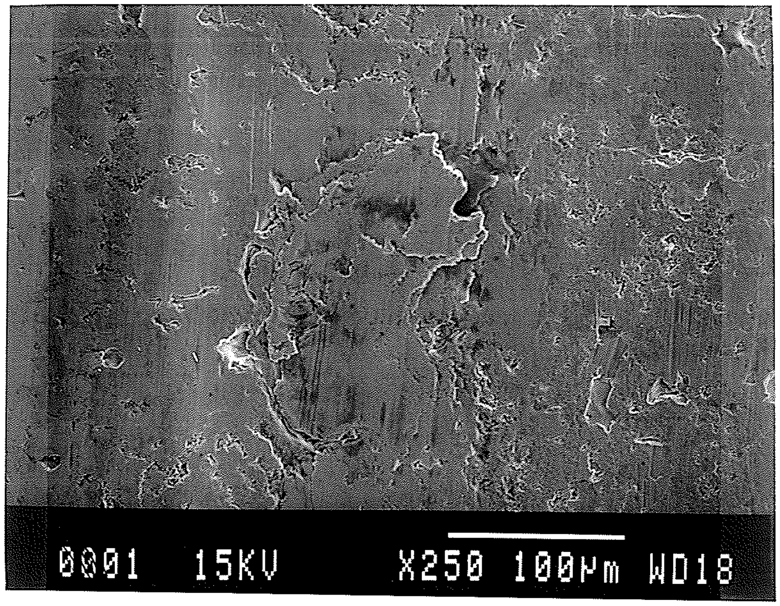

Figure 5.9: Worn surface of AS2 after 60 minutes of sliding

It can be noted from these figures that the grinding marks apparent in Figure 5.7 diminish gradually, with increasing sliding time (Figures 5.8-5.9). The surface at this stage appears to have undergone polishing wear. Simultaneous wear rate was very small and indicates mild wear.

The above state changed almost abruptly, after 80 minutes of sliding, when fatigue cracking (pitting) (Figure5.10a-b) and removal of coating material by fracture (5.10b-c) was noticed. At the same time "lips" of deformed material appeared on the surface (Figure 5.10c). These lips were "ironed" out due to subsequent deformation during the next 15 minutes of sliding. The layers of deformed material so formed can be seen in Figure 5.11. The wear rate of both the pin and the specimen increases substantially during the same period. As a result, the pin apparent contact area becomes equal to its nominal contact area. The most severe wear is noted in the next (and final)

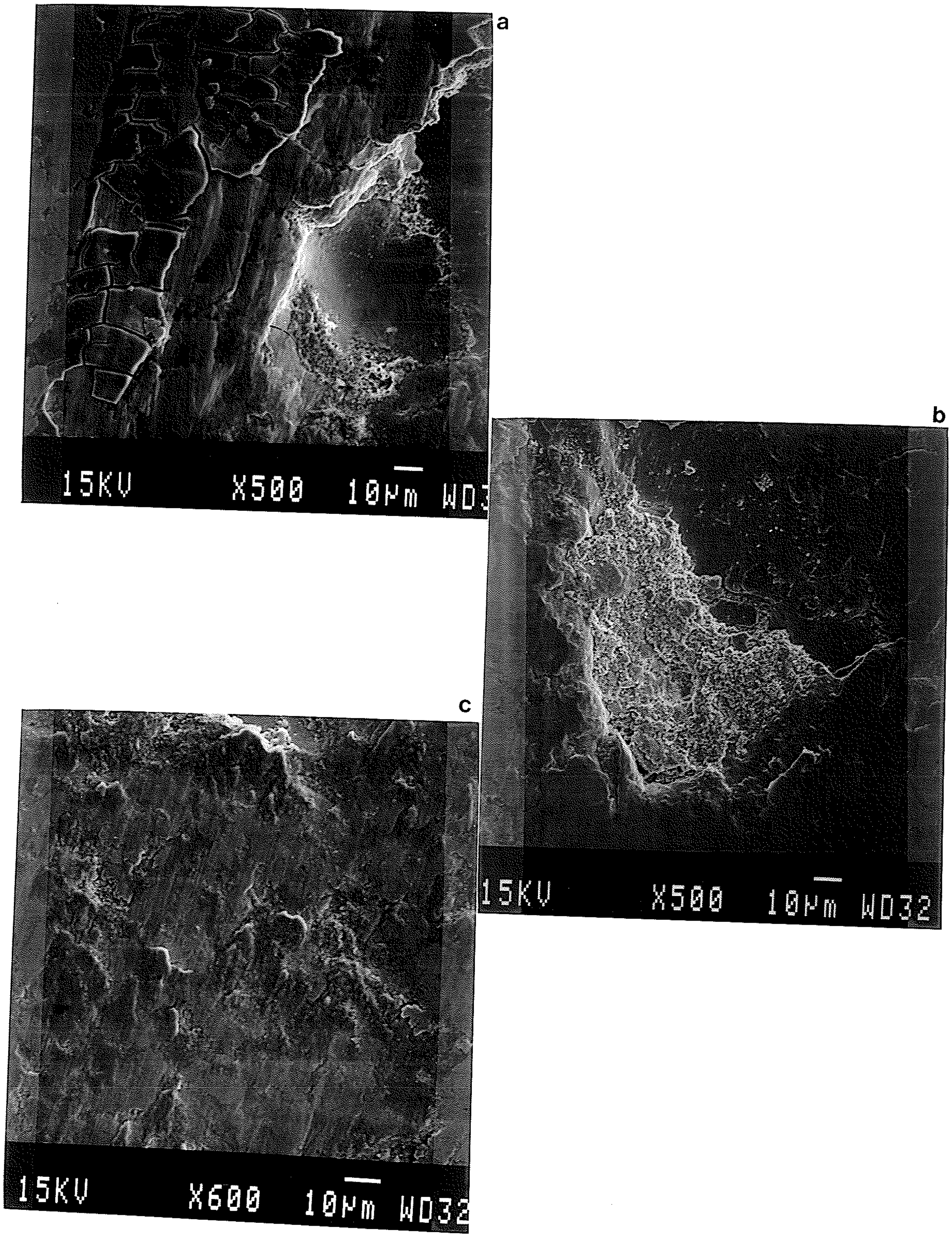

Figure 5.10: Worn surface of AS2 after 80 minutes of sliding

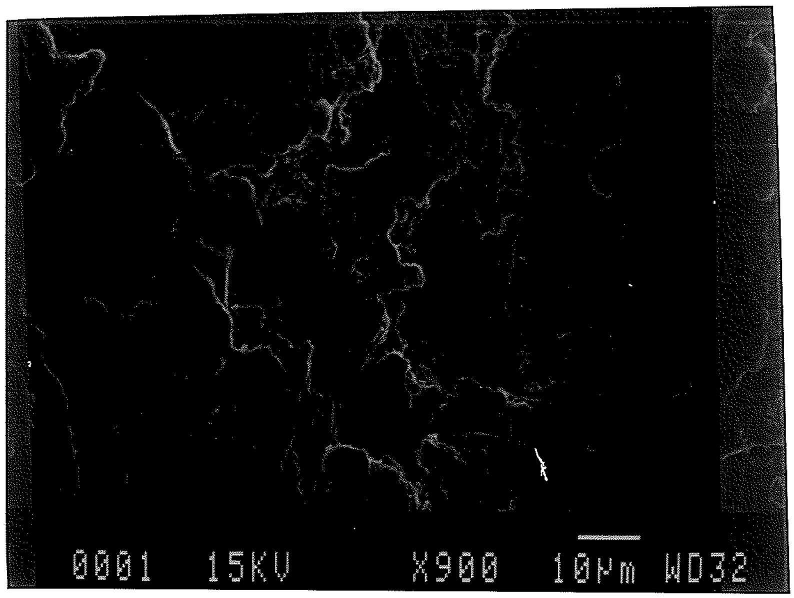

Figure 5.11: Worn surface of AS2 after 95 minutes of sliding

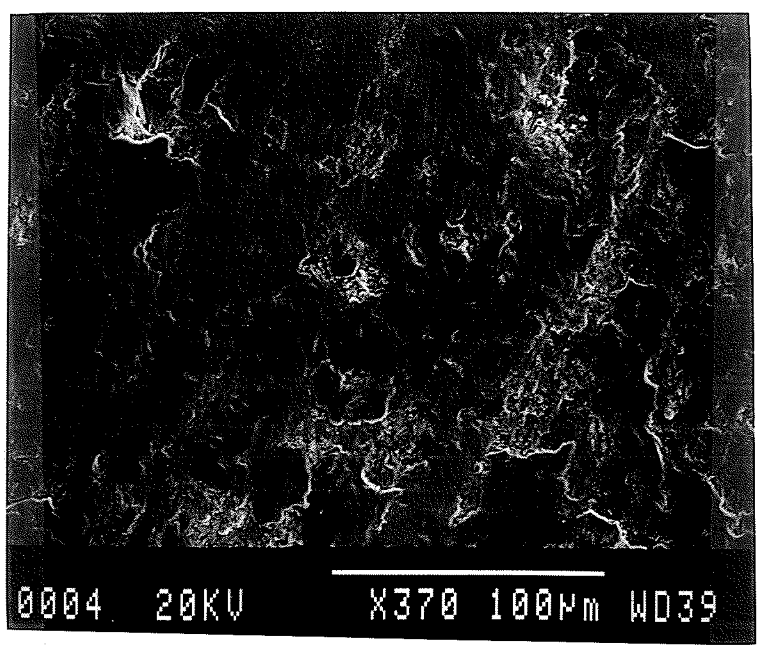

Figure 5.12: Worn surface of AS2 after 99 minutes of sliding

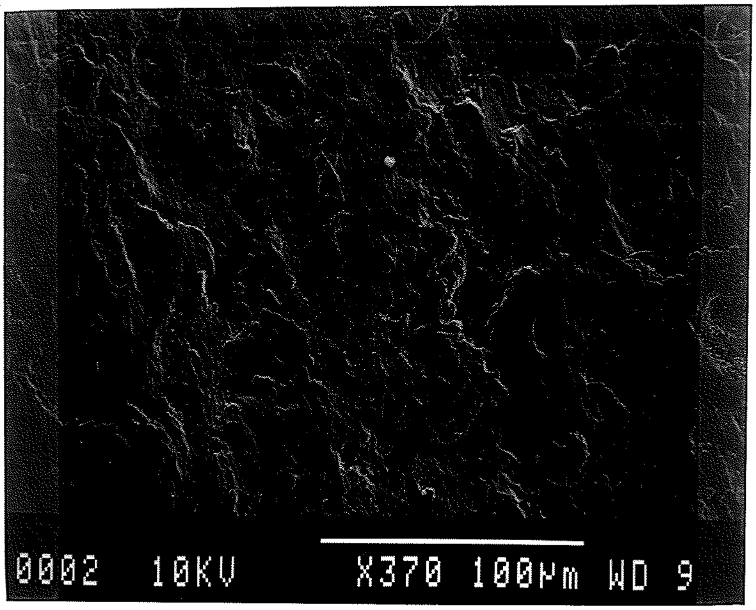

Figure 5.13: Worn surface of AS1 after 89 minutes of sliding

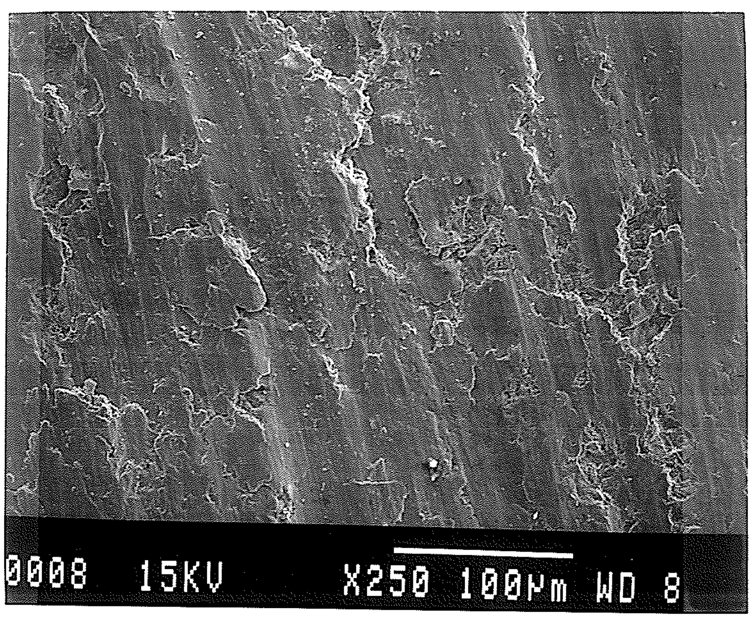

Figure 5.14: Worn surface of AS3 after 115 minutes of sliding

four minutes of sliding wear (Figure 5.12). This wear manifests itself in widespread particle removal, deformation and grooving.

The same sequence of mild (gradual) and severe wear was observed in the other two specimens (used in tests S1 and S3); only the time taken for transition between wear mechanisms varied. While in AS1, severe deformation, grooving and fracture were noticed after 85 minutes of sliding(Figure 5.13), in AS3 the same were noticed after 115 minutes of sliding(Figure 5.14). In the latter two cases too, severe wear was noticed to occur with an increase in apparent contact area between the specimen and the pin. This further substantiates the deduction that dramatic increase in contact area causes a change in wear mechanism.

The characterization of the pins was also carried out under the SEM. The roughness of the pin surfaces, however, could not be determined due to their small size. The SEI of the pins are given in Figures 5.15–5.16. The as-ground surface of the pins, prepared for the wear tests, appeared very smooth, visually as well as microscopically (Figure 5.15). In the same figure, however, surface pores could be noticed. These pores are thought to have been caused by the pulling out of the nodular graphite during the surface grinding operation. The surface of the pin CI2 used in test S2 shows evidence of severe wear after the final four minute sliding interval. The SEI of this pin, Figure 5.16, shows evidence of plastic deformation, particle removal by fracture and grooving. SEI of wear debris after the final four minute sliding interval during test S2 are given in Figure 5.17. While, in Figure 5.17a a particle fractured from the surface of the coating can be seen, in Figure 5.17b a particle formed by the agglomeration of two or more primary particles can be seen.

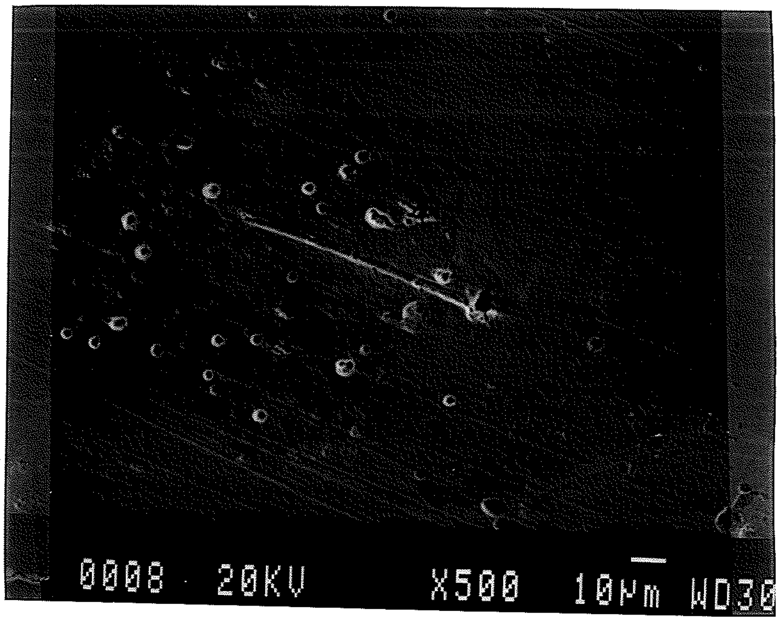

Figure 5.15: Typical as-ground surface of pins before wear testing

The figures 5.7–5.17 indicate the occurrence of the following sequence of events during the unlubricated, reciprocating, sliding wear of arc-sprayed martensitic stainless steel coating against a martensitic nodular cast iron pin:

The initial low wear in the specimens occurs during simple alignment improvements, before the establishment of a uniform and stable contact geometry between the sliding surfaces. This is followed by a rapid wear-in period during which excessive debris generation takes place. The final period is the scuffing period, characterized by high noise levels, vibrations in the apparatus, stick-slip motion and rising specimen bulk temperatures.

As pointed out in a much detailed review [36], scuffing in the present research program is preceded by pitting (Figure 5.10a-b) and mild adhesive wear (Figure 5.10c). The wear surface due to scuffing shows signs of scoring and a series of grooves and

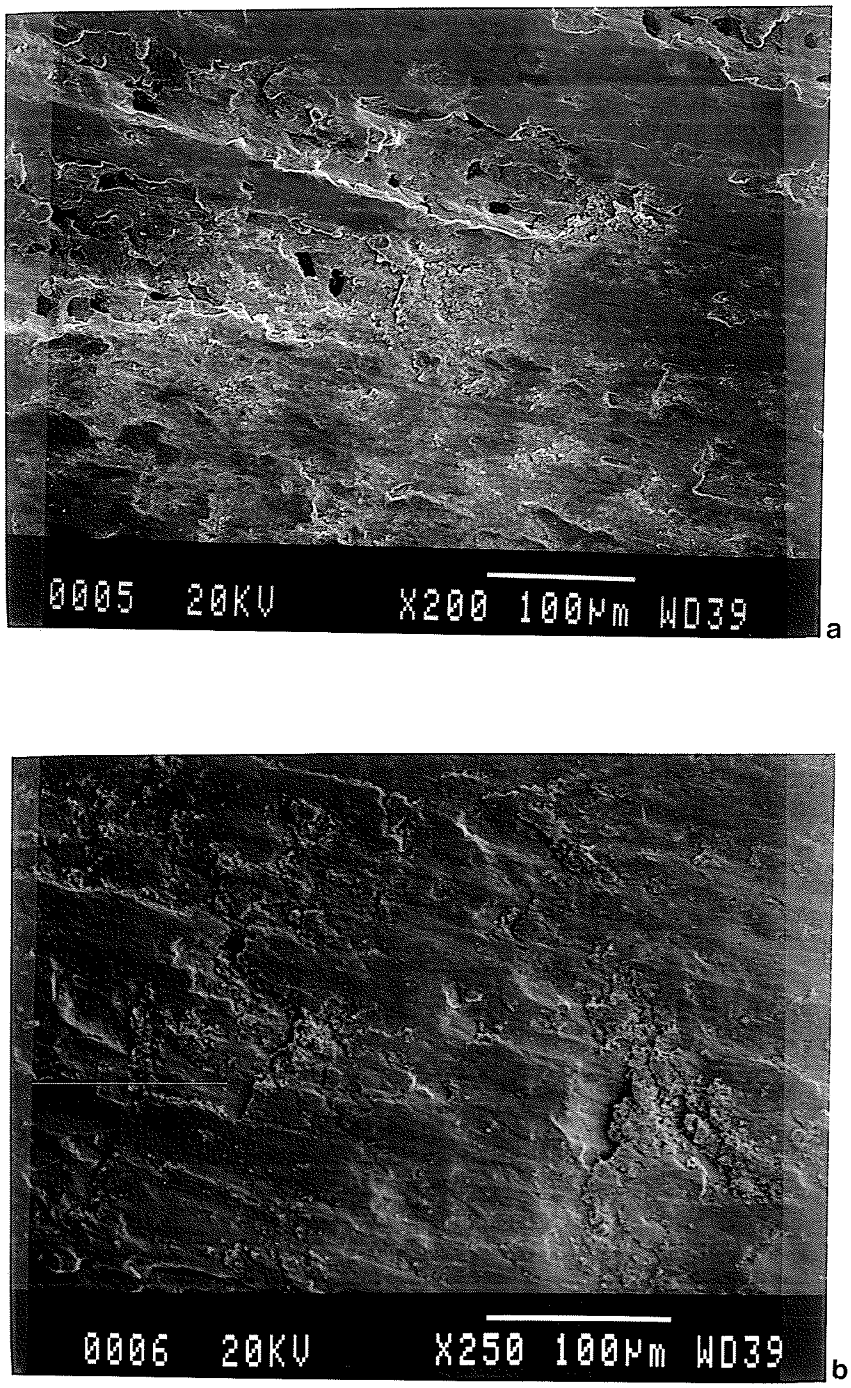

Figure 5.16: Worn surface of pin used on AS2 after 99 minutes of sliding

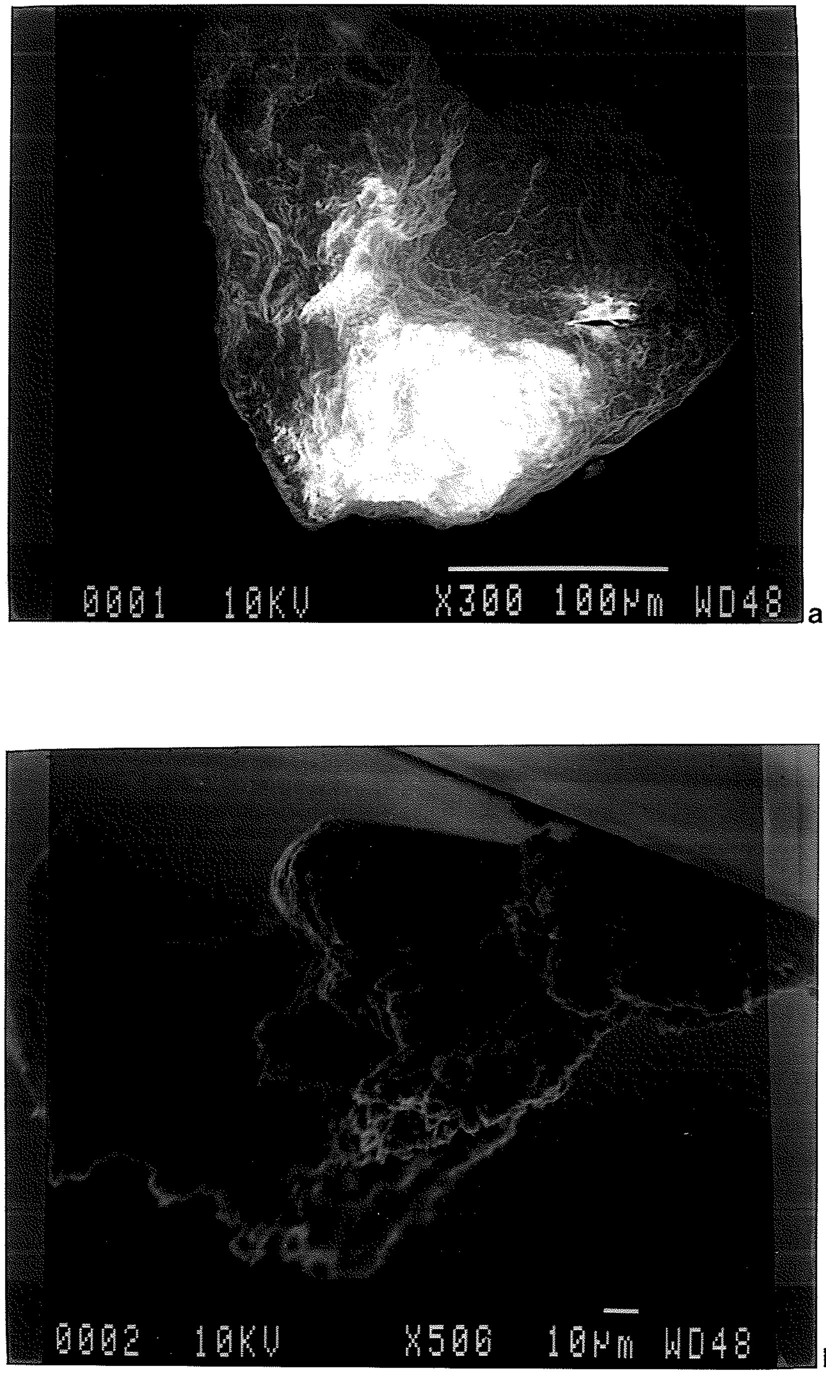

Figure 5.17: Wear debris collected from test S2 after the sixth (4 min) sliding interval

ridges in the surface, oriented in the sliding direction (Figures 5.13–5.14,5.16).

The excessive wear debris is thought to have caused a quick rise in friction and hence a rise in the bulk specimen temperature. In a recent work [23], the role of the generation and trapping of such wear debris in the rise of friction has been discussed. The high friction in the present work was, however, not seen to cause any local melting or "welding." Simultaneously, adhesive wear as "conventionally" assumed to occur by the presence of "welded" or transferred material particles was not observed. The relative rest between the sliding components, during stick slip, is then thought to be caused by the mechanical interlocking of valleys and ridges in the severely deformed specimen and pin surfaces or due to wedge formation. The importance of wear debris in both of the above can be readily pointed out. While, wear debris is known to cause abrasive wear, as characterized by grooves, ridges and valleys, it is also considered an important factor in wedge formation. As pointed out in chapter 3, abrasive wear and wear debris production are mutually dependent processes, until the generation of high friction. At such a stage, melting or severe deformation and processes resulting from the same, cause severe wear. Scuffing is one of them. Needless to say, the involvement of preceding abrasion in scuffing is ubiquitous. This is in accordance with the mechanisms proposed in the literature and the fact that adhesion is thought to be only one of several factors involved in sliding wear. Since the sliding surfaces are made of similar material, the type of stick-slip motion can be given by Figure 3.6. This was also observed during experiments in the present work.

The generation of copious amounts of wear debris can be explained by drawing a relationship between the sequence of events in the wear tests described above and a recent wear classification scheme [41]. After the completion of geometrical alignment and the rapid wear-in period, the apparent nominal contact stress between the sliding surfaces was approximately 8MPa. At the sliding velocity of approximately 0.4 m/s, it gave a sliding regime of high stress and medium velocity. According to the above stated work [41], this lies in the severe wear regime. In this regime, the frictional traction, as pointed out earlier, causes a catastrophic increase in the plastic shear strain accumulated in the subsurface layer. This causes the nucleation and growth of sub-surface cracks which eventually break out to give wear debris. Some of this debris undergoes changes in shape and size during subsequent entrapment between the sliding surfaces. As a result, agglomeration of individual debris particles may occur. This may produce debris like that shown in Figure 5.17b.

Thus, it is demonstrated that the debris produced during the polishing and subsequent run-in of the sliding surfaces, in the present work, is the main contributor to an increase in frictional traction between the said surfaces. This causes more severe abrasive wear and further generation of wear debris. A combination of these factors leads to scuffing wear of the surfaces. Such wear is very severe and invariably leads to seizure. In lubricated wear tests conducted as part of this study, however, very mild wear was observed. The results from these tests are reported and discussed below.

5.6.2 Comparative Tests Objective

The lubricated wear tests were performed on the three coatings - AS, PC and EC, under the same lubrication condition and the same piston ring (CI) for 200,000 cycles. The applied load was varied from 98N to 392N. For each loading condition, loss in the mass of the coating and CI was determined using the techniques described earlier.The mass loss of the coating material as a function of applied load for the three coatings is plotted in Figure 5.18a. For each case, the loss in the mass of CI is plotted in Figure 5.18b. The actual values of volume loss for these tests are given in appendix D.

The sum of the loss in mass of the coating and the corresponding CI mass loss is plotted in Figure 5.18c. In reality, it is the combined performance of both the mating surfaces that provides a true measure of wear. Figure 5.18 indicates that the mass

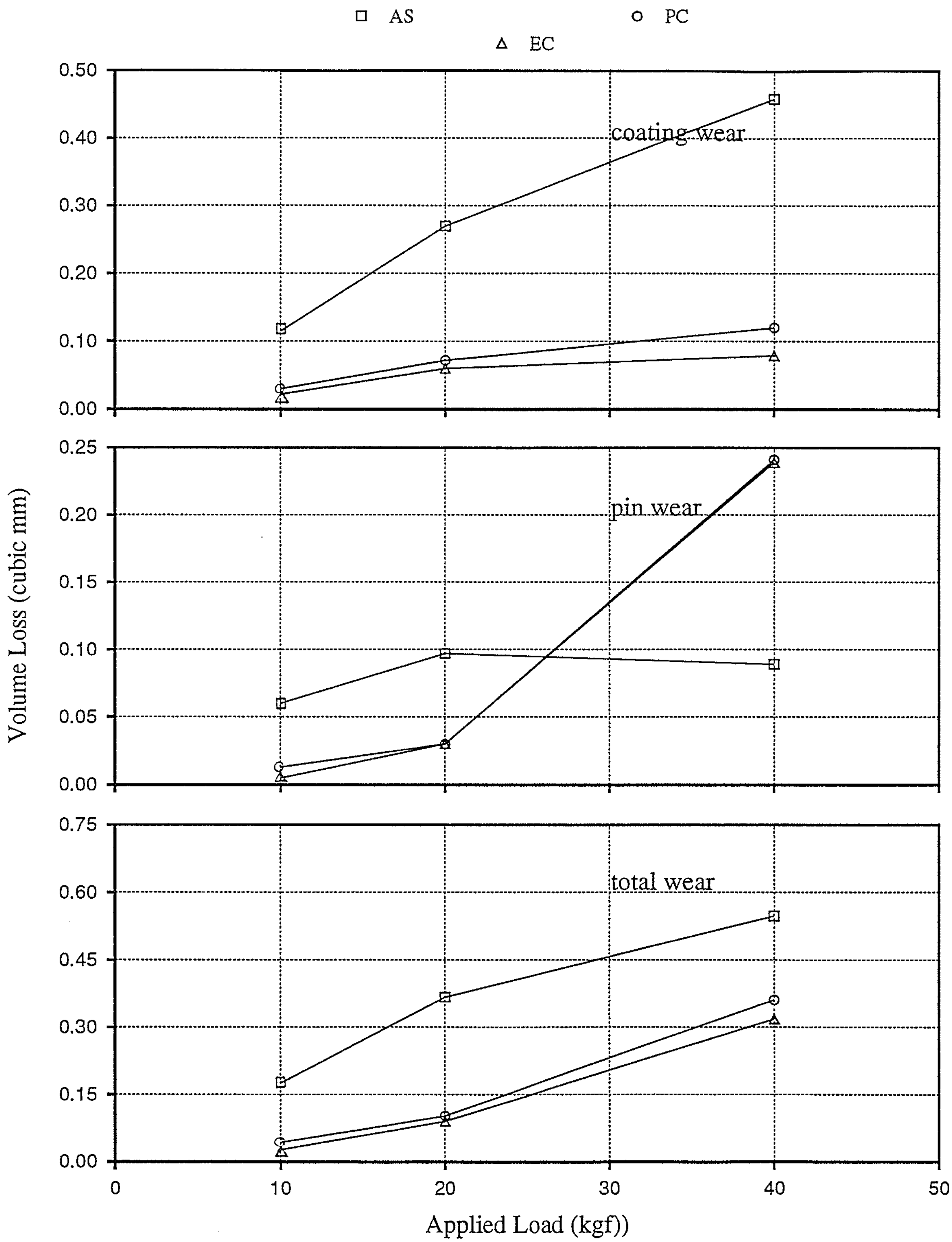

Figure 5.18: Volume loss of material after 200 000 cycles of lubricated wear tests

loss of the AS coating is higher than that of the other two coatings at all the load levels. In the case of mass loss of the piston ring sliding against AS, the value at the 392N load level does not rise as dramatically above the 196N load level as it does during sliding against the other two surfaces, which are also considerably harder than AS.

From the above figures, it can also be noticed that PC and EC performed equally well and both performed better than AS. The scanning electron images (SEI) of the wear surface of the coatings after 200,000 cycles of wear test at 392N load are given in Figure 5.19. The wear surface of AS [Figure 5.19a] was observed to have abrasive grooves (A), plastic flow (region near B) and wear debris compaction (C). Energy dispersive x-ray analysis (EDX), on the SEM, revealed the presence of CI material in this debris. The amount or fraction of this CI material could not be ascertained. However, the fraction of abrasive groove area to wear scar area was qualitatively estimated to be quite small.

In the case of PC [Figure 5.19b], it was observed that the wear was mainly due to mild abrasion or polishing (A). The evidence of any deep scratching or material transfer was not found. The polishing effect was also observed in EC: Figure 5.19c shows the unworn portion (A), the polished portion (B) and a smooth groove (C). Typical wear surface profiles obtained from the profilometer are given in Figure 5.20. It can be noticed that the profiles of the worn thermally sprayed coatings (a and b) contain many sharp dips indicating the porous nature of the coatings. The hard chrome, on the other hand, was comparatively smoother in the worn groove.

The role of surface porosity in reducing wear can be discussed in light of its ability to act as a reservoir for lubricant and/or wear debris. The role of lubricant in reducing severe wear has been discussed earlier. Hence, surfaces, such as the ones used in the present work, which can retain lubricant can have lesser wear than those which do not. Moreover, the entrapment of wear debris in the surface pores makes them unavailable

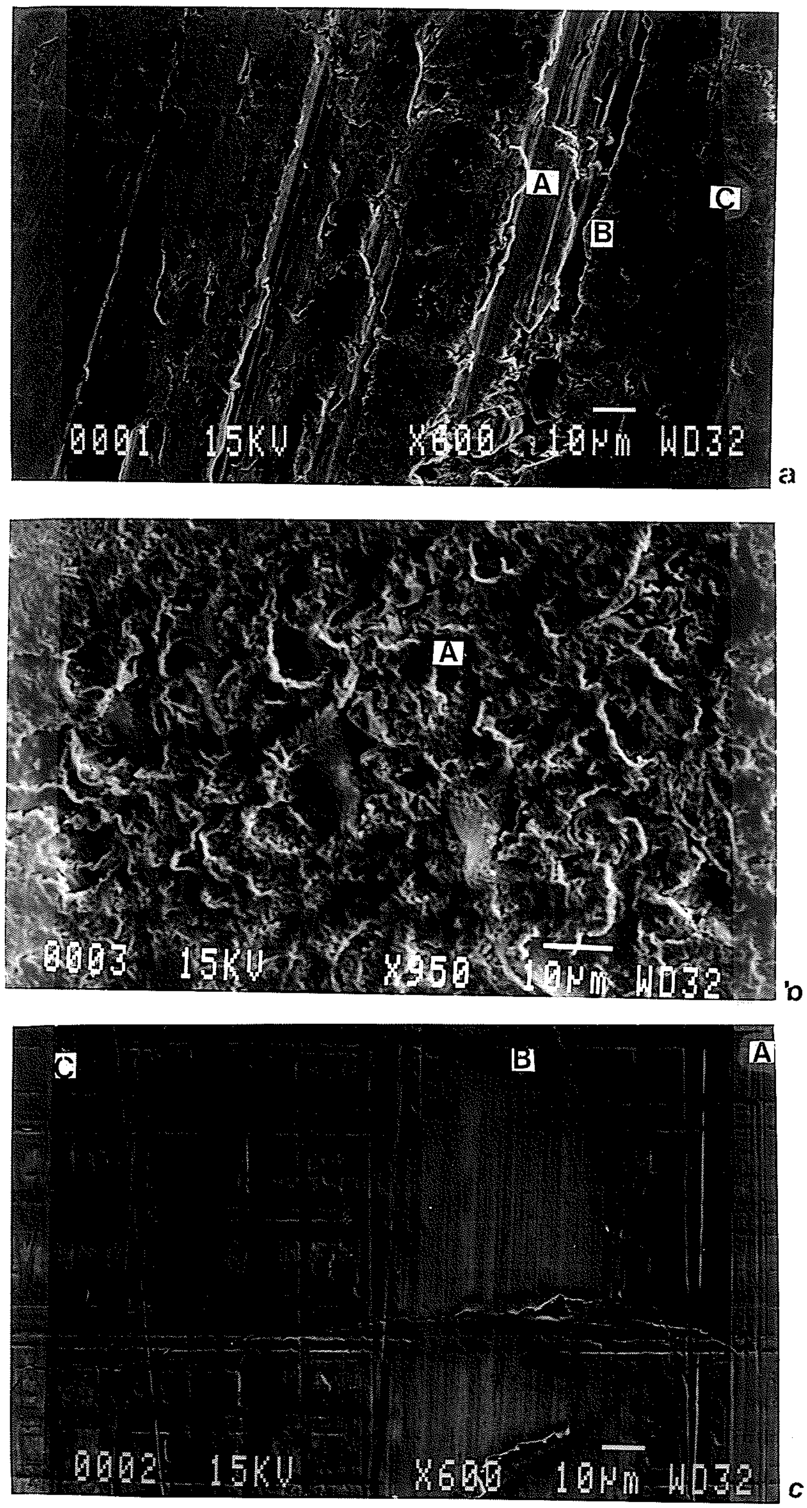

Figure 5.19: Worn surface after 200 000 cycles of lubricated wear tests; (a): AS, (b): PC and (c): EC

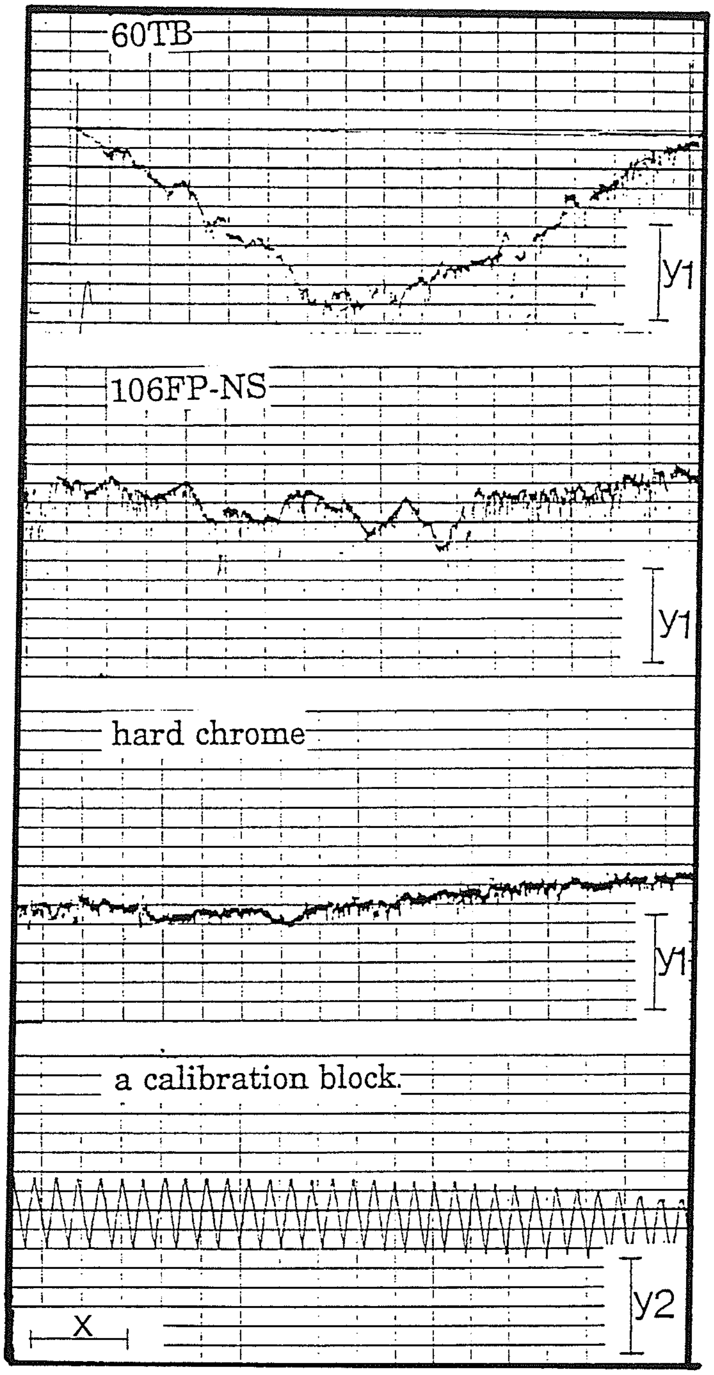

LEGEND

x = 0.125 mm
y1 = $3.125 * 10^{-3}$ mm
y2 = $3.125 * 10^{-2}$ mm

Figure 5.20: Typical surface profile outputs from the profilometer, after 200 000 cycles of lubricated wear tests

for causing abrasive wear. Furthermore, it is thought that whatever little debris is generated gets carried along the inclined specimen and helps in reduced wear. Thus, the available debris causes only mild wear.

A comparison of the lubricated sliding wear of AS with that of carbon steel [35] indicates some similarities in the flow wear pattern of the two cases. In both the cases, thin layers are extruded in the side direction by plastic flow of surface layers at the local spots of contact between the mating surfaces. However, no overlap of extruded layers from opposite layers was observed in the present case. Hence, the formation of loose wear debris due to the overlap of these layers, as observed in the case of carbon steel can be ruled out here. The major portion of wear debris in the case of AS is thought to have been generated by the fracture of surface asperities, as evidenced by micropitting in the surface profile of the wear scar [Figure 5.20a].

Due to the high contact stresses, the wear debris could be deformed and compacted into the surface cavities. The effect of any local heating on subsequent melting and deforming of wear surface asperities or the wear debris could not be ascertained. Since, no adhesive wear or severe abrasive wear was observed, the role of lubricant in preventing high wear rates and severe wear mechanisms, as reported earlier, was confirmed. The limited number of abrasive grooves are thought to have been caused when a surface particle (such as a spalled asperity or a microchip) ploughed a furrow through the surface. The compacted wear debris is thought to have contributed to the smoothing of the wear scar [Figure 5.19a].

In the case of PC, mild polishing was noticed. High magnifications were required to resolve the details of the polishing wear processes. One of the reasons that may have contributed to reducing wear of PC, could be its high hardness values. The role of toughness of PC, in determining its rate of wear, could not be quantitatively determined. However, qualitatively, the evidence for the same was not observed. The latter deduction results from the observed absence of signs of fracture on the wear surface. The only apparent wear is caused by the repeated polishing action of the piston ring.

The wear of the EC coating appears to have a combination of polishing and mild abrasion. These effects can be noticed in Figure 5.20c. The surface of the specimen has undergone some polishing (B). The smooth groove (C) has formed due to the grinding action, of a spalled asperity trapped between the mating surfaces under the high stress. The piston ring wear was mainly due to abrasive action of hard surface asperities and any loosened surface particles trapped between the mating surfaces. Whatever debris that was generated, either contributed to the polishing action (mild abrasion), or got collected in the surface micropits or was carried away with the lubricant flow, as in the case of PC.

Surface porosity, in thermally sprayed coatings, was noticed to have contributed beneficially to reduced wear in lubricated tests in the present work. It was thought that it was beneficial due to its ability for improved lubricant retention and for providing reservoirs for collecting the wear debris.

Chapter 6

CONCLUSIONS

1. A wear test set-up for simulating lubricated, reciprocating, sliding wear was fabricated and successfully tested. Having the rig at an incline reduces excessive friction due to wear debris, at the same time allowing the presence of some debris.

2. No definite conclusion about the dependence of wear on either the time of sliding or the area of contact between the surfaces could be made.

3. The wear in arc-sprayed martensitic stainless steel coating could be related to wear in similar metal systems. Moreover, it was found that under conditions of high load and medium velocity, abrasive, adhesive and pitting wear precede scuffing wear. The order of occurrence of the preceding wear mechanisms is not clear. Though, simultaneous action and mutual dependence of the three can not be ruled out.

4. In lubricated tests, the performances of plasma-sprayed Cr_2O_3 and hard chrome were found to be comparable. Surface polishing (mild abrasion) of the coating and abrasive wear of the piston ring were the major contributors to the wear in

these two coatings.

5. In lubricated tests, the wear of arc-sprayed martensitic stainless steel was more than that of the other two coatings. This could be attributed to greater ductility of the former. The major modes of wear for the steel were plastic deformation and ploughing (abrasive action). The wear debris compacted in the surface cavities contributed to a smoothing of the surface.

6. In lubricated tests, the surface porosity was observed to act as a reservoir for lubricant and wear debris which helped in preventing wear mechanisms responsible for causing severe wear.

REFERENCES

[1] Nadel, J. and Eyre, T.S., "Cylinder Liner Wear in Low Speed Diesel Engines," Tribology International, Oct. 1978, p. 267.

[2] El-Sherbiny, M.G., "Cylinder Liner Wear," Proc. 9th Leeds-Lyon Symposium on Tribology, Leeds, England, Sept. 7-10, 1982, p. 182.

[3] Jones, A.R., "Microcracks in Hard Chromium Electrodeposits," Plating and Surface Finishing, April 1989, p. 62.

[4] Gawne, D.T., and Ma, U., "Friction and Wear of Chromium and Nickel Coatings," Wear, Vol. 129, No. 1, 1989, p. 123.

[5] Usmani, S. and Tandon, K., "Evaluation of Thermally Sprayed Coatings Under Lubricated Reciprocating Wear Conditions," 1992 (submitted for publication).

[6] Tandon, K., Usmani, S., Chaturvedi, M.C. and Cahoon, J.R., "Locomotive Diesel Engine Cylinder Liner Coatings: Phase I – Evaluation of Thermally Sprayed Coatings," Transport Canada Report No. TP11067E, Montreal, PQ, July 1991.

[7] Herman, H., "Coatings and Coating Practice," Advanced Materials and Processes, Vol. 137, No. 1, Jan. 1990, p. 59.

[8] Herman, H.," Plasma-Sprayed Coating," Scientific American, Vol. 259, No. 3, Sept. 1988, p. 112.

[9] Kubel Jr., Edward J., "Thermal Spraying Technology: From Art to Science," Advanced Materials and Processes Inc., Metal Progress, Dec. 1987, p. 69.

[10] Longo, F.M., Chairman, "Proc. ASM's Second National Conf. on Thermal Spray," Long Beach, CA, Oct. 31-Nov. 2, 1984.

[11] Houck, D.L., "Proc. National Thermal Spray Conference," Cincinnati, OH Oct. 24 - 27, 1988.

[12] Thorpe, M.L., "Recent Advances in Arc Coating Technology and Equipment," Proc. ASM's II National Conf. on Thermal Spray, Long Beach, CA, Oct. 31-Nov. 2, 1984, p. 91.

[13] Nusum, C., "Applications in Thermal Spraying," Proc. National Thermal Spray Conference, Cincinnati, OH Oct. 24 - 27, 1988, p. 449.

[14] Mcpherson, R., "A Review of Microstructure and Properties of Plasma Sprayed Ceramic Coatings,"Surface and Coatings Technology, Vol. 39/40, 1989, p. 173.

[15] Harris, S.J., Cifuentes, L., Cobb, R.C. and James, D.H., "Influence of Heat Transfer on the Structure and Properties of Arc Sprayed Low Alloy Steels," Proc. First Int'l Conf. on Surface Engineering, Brighton, UK, June 25-28, 1985, p. 79.

[16] Suzuki, Y., Tanoue, S. and Yamaguchi, H., "Ceramic Coating on Engine Parts," Proc. ASM's Int'l Conf. on Surface Modifications and Coatings, Toronto, ON, Canada, Oct 14-16, 1985.

[17] Suzuki, Y., "Surface Modifications of Pistons and Cylinder Liners," Proc. ASM's International Conf. on Surface Modifications and Coatings, Toronto, ON, Canada, Oct. 14-16, 1985.

[18] Murthy, A.K., Komvopoulos, K. and Brown, S.D., "Processing and Characterization of Multi-Layered Wear-Resistant Ceramic Coatings," Trans. ASME., J. Eng. Materials and Technology, Vol. 112, April 1990, p. 164.

[19] Dufrane, K.F. and Glasser, W.A., "Wear of Ceramics in Advanced Heat Engine Applications," Proc. Int. Conf. on Wear of Materials, Houston, TX, April 5-9, 1987, p. 285.

[20] Aronov, V., Mesyef, T., "Wear in Ceramic/Ceramic and Ceramic/Metal Reciprocating Sliding Contact, Part 1," Trans. ASME, Journal of Tribology, Vol. 108, Jan. 1986, p. 16.

[21] Fischer, T.E., "Friction and Wear of Ceramics," Scripta Met. Mater., Vol. 24, 1990, p. 833.

[22] Rosenfield, A.R., "Wear and Fracture Mechanics: Are they Related?," Scripta Met. Mater. Vol. 24, 1990, p. 811.

[23] Ajayi, O.O. and Ludema, K.C., "Mechanism of Transfer Film Formation During Repeat Pass Sliding of Ceramic Materials," Wear, Vol. 140, No. 2, Nov. 1990, P. 191.

[24] Wang,H.G. and Herman, H., "Structure and Properties of Plasma Sprayed Spinel," Cer. Bull., Vol. 68, No. 1, 1989, p. 97.

[25] Ritchie, Jack, "Selecting Thermal Spray Coatings for the Repair of Equipment Parts by the Job Shop," Proc. ASM's II National Conf. on Thermal Spray, Long Beach, CA, Oct. 31-Nov. 2, 1984, p. 87.

[26] Halling, J., "Introduction to Tribology," Wykeham Publications (London) Ltd., London and Winchester, 1976.

[27] Czichos, Horst, "Tribology, A Systems Approach to the Science and Technology of Friction, Lubrication and Wear," Elsevier Scientific Publishing Company, New York, 1978.

[28] Peterson, M.B., "Wear Testing Objectives and Approaches, " in Selection and Use of Wear Tests for Metals , STP 615, ASTM, 1976.

[29] Rigney, D.A., "Viewpoint Set on Materials Aspects of Wear–Introduction," Scripta Met., Vol. 24, No. 5, 1990, p. 799.

[30] Budinski, Kenneth G., "Surface Engineering for Wear Resistance," Prentice Hall, New Jersey, 1988.

[31] Kayaba, T., Hokkirigawa, K. and Kato, K., "Analysis of the Abrasive Wear Mechanism by Succesive Observations of Wear Processes in a Scanning Electron Microscope," Wear, 110 (1986), p. 419.

[32] Lancaster, J.K., "Material-Specific Wear Mechanisms: Relevance to Wear Modelling," Wear, Vol. 141, 1990, p. 159.

[33] Tabor, D., " Friction and Wear Developments Over the Last Fifty Years," Conf. Proc. I Mech. E, 1987, p. 157.

[34] Chang, Y.J. and Wilsdorf, D.K., "A Case of Wear Particle Formation Through Shearing-Off at Contact Spots Interlocked Through Microroughness in Adhesive Wear," Wear. 120 (1987), p. 175.

[35] Akagaki, T. and Kato, K., "Wear Mode Diagram in Lubricated Sliding Friction of Carbon Steel," Wear, Vol. 129, 1989, p. 303.

[36] Dyson, A., "Scuffing," in Treatise on Mater. Sci. and Tech., ed. D. Scott, Vol. 13, Academic Press, New York, 1979, p. 175.

[37] Lim, S.C., Ashby, M.F., and Brunton, J.H., "Wear-Rate Transitions and Their Relationship to Wear Mechanisms," Acta Metall., Vol. 35, No. 6, 1987, p. 1343.

[38] Sarkar, A.D., "Wear of Metals," International Series in Mater. Sci. and Tech., ed. J. Halling, Vol. 18, Pergamon Press, New York, p. 32.

[39] Lim, S.C. and Ashby, M.F., "Wear Mechanism Maps," Acta Metall., Vol. 35, No. 1, 1987, p. 1.

[40] Archand, J.F. and Hirst, W., "Proc. Royal Society," Ser. A, 236, 1956, 397.

[41] Ashby, M.F. and Lim, S.C., "Wear-Mechanism Maps," Scripta Met. Mater., Vol. 24, 1990, p. 805.

[42] Bayer, R.G., "Wear Testing," in Metals Handbook, 9th edn., Vol. 8: Mechanical Testing, 1990, p. 601.

[43] Fein, R.S., "Boundary Lubrication," in Handbook of Lubrication, ed. E. Richard Booser, CRC Press, Boca Raton, Florida, 1983.

[44] Rowe, C.N., "Lubricated Wear," in Handbook of Lubrication, CRC Press, Boca Raton, Florida, 1983.

[45] Barber, G.C. and Ludema, K.C., "The Break-in Stage of Cylinder-Ring Wear: A Correlation Between Fired Engines and a Laboratory Simulator," Wear, Vol. 118, 1987, p. 57.

[46] Rabinowicz, E., "Penetration Hardness and Toughness Indicators of Wear Resistance," Proc. I. Mech. Eng., Vol. I, 1987, p. 197.

[47] Lewis, C.F., "Rubbing Materials the Right Way," Materials Engineering, March 1991, pp. 31.

[48] Czichos, H., Becker, S. and Lexow, J., "International Multilaboratory sliding wear tests with Ceramics and Steel," Wear, 135 (1989), pp. 171.

[49] ASTM Standard G77–83.

[50] ASTM Standard G83–89.

[51] ASTM Standard G99–90.

[52] Ruff, A.W., "Comparison of Standard Test Methods for Non-Lubricated Sliding Wear," Wear, Vol. 134, 1989, p. 49.

[53] Chiou, Y-C and Kato, K., "Wear Mode of Micro-Cutting in Dry Sliding," Jour. JSLE, Int'l Edn., No. 9, 1988, p. 17.

[54] Quinn, T.F.J., "The Thermal Aspects of Wear in Tribotesting," Proc. Conf. I.Mech.E. 1987, Vol. I, p. 253.

[55] Hogmark, S., Vingsbo, O. and Fridstrom, S., "Mechanisms of Dry Wear of Some Martensitic Steels," Wear, 31, 1975, p. 39.

[56] Zhang, X., Zhang, C. and Zhu, C., "Slip Amplitude Effects and Microstructural Characteristics of Surface Layers in Fretting Wear of Carbon Steel," Wear, 134, 1989, p. 297.

[57] Zum-Gahr, K.H., " Sliding wear of Ceramic-Ceramic, Ceramic-Steel and Steel-Steel Pairs in Lubricated and Unlubricated Contact," Wear, 133, 1989, p. 1.

[58] Chetwynd, D.G., "The Measurement of Wear Damage," Proc. I Mech Eng, Vol. 201, No. C4, 1987, p. 251.

[59] Czichos, H. and Habig, K-H, "Wear of Medium Carbon Steel: A Systematic Study of the Influences of Materials and Operating Parameters," Wear, 110, 1986, p. 389.

[60] Blann, G.A., Diaz, D.J. and Nelson, J.A., "Raising the Standards for Coating Analysis," Advanced Materials and Processes, Dec. 1989, p. 31.

[61] Kretzschmar, E., "Methods of Testing Sprayed and Ceramic Coatings," Surfacing Journal, Jan. 1977, p. 2.

[62] Beltzung, F., Zambelli, G., Lopez, E. and Nicoll, A.R., "Fracture Toughness Measurement of Plasma Sprayed Ceramic Coatings," Thin Solid Films, 181, 1989, p. 407.

[63] Brown, S.D., Chapman, B.A. and Wirtz, G.P., "Fracture Kinetics and the Mechanical Measurement of Adherence," Proc. National Thermal Spray Conference, Cincinnati, OH Oct. 24 - 27, 1988, p. 147.

[64] ASTM Standard B765-86.

[65] Kang, S.C. and Ludema, K.C., "The "Breaking-In" of Lubricated Surfaces," in K.C. Ludema (ed.), Proc. Int. Conf. on Wear of Materials, April 14-18, 1985, ASME, New York, 1985.

[66] Wang, H.G., Fischman, G.S. and Herman, H., "Plasma-Sprayed Cordierite: Structure and Transformations," Jour. Mater. Sci., 24, 1989, p. 811.

[67] Rigney, D.A., "Sliding Wear of Metals," Ann. Rev. Mater. Sci., Vol. 18, 1988, p. 141.

[68] ASTM Standard C633-79$^{\epsilon 1}$.

APPENDIX A

```
CHARACTER*10 SWdata,PWdata, TWdata
INTEGER ISW
PRINT*, "WHAT IS THE NAME OF THE FIRST FILE?"
READ(*,*) SWdata
PRINT*, 'WHAT IS THE NAME OF THE SECOND FILE?'
READ(*,*) PWdata
PRINT*, 'WHAT IS THE NAME OF THE THIRD FILE?'
READ(*,*) TWdata
PRINT*, 'TYPE 0 FOR ADD, 1 FOR SUBTRACT, 2 FOR REPLACING X OF '
PRINT*, 'FIRST FILE BY THAT OF SECOND, 3 FOR REPLACING Y OF '
PRINT*, 'FIRST FILE BY THAT OF SECOND '
READ(*,*) ISW
OPEN(UNIT=80,FILE=SWdata)
OPEN(UNIT=70,FILE=PWdata)
OPEN(UNIT=60,FILE=TWdata)
IF(ISW.EQ.0)THEN
WRITE(60,*)'C SUM of the data of ',SWdata,'and ',PWdata
PRINT*, 'ADDING ',SWdata, 'AND ', PWdata
PRINT*, 'output file name is : ', TWdata
DO 10 I=1,6
CALL RDCMNT1
READ(80,*) X1,A1,X2,A2,X3,A3,X4,A4
CALL RDCMNT2
READ(70,*) X1,B1,X2,B2,X3,B3,X4,B4
C1=A1+B1
C2=A2+B2
```

```
C3=A3+B3
C4=A4+B4
WRITE(60,30) X1,C1,X2,C2,X3,C3,X4,C4
30 FORMAT('',8(F8.3))
10 CONTINUE
ENDIF
IF(ISW.EQ.1)THEN
WRITE(60,*)'C DIFFERENCE of the data of ',SWdata,'and ',PWdata
PRINT*, 'SUBTRACTING ',SWdata, 'AND ', PWdata
PRINT*, 'output file name is : ', TWdata
DO 20 I=1,6
CALL RDCMNT1
READ(80,*) X1,A1,X2,A2,X3,A3,X4,A4
CALL RDCMNT2
READ(70,*) X1,B1,X2,B2,X3,B3,X4,B4
C1=A1-B1
C2=A2-B2
C3=A3-B3
C4=A4-B4
WRITE(60,30) X1,C1,X2,C2,X3,C3,X4,C4
20 CONTINUE
ENDIF
IF(ISW.EQ.2)THEN
WRITE(60,*)'C REPLACED X OF ',SWdata,'by X of ',PWdata
PRINT*, 'Replacing ',SWdata, 'AND ', PWdata
PRINT*, 'output file name is : ', TWdata
DO 40 I=1,6
```

```
CALL RDCMNT1
READ(80,*) X1,A1,X2,A2,X3,A3,X4,A4
CALL RDCMNT2
READ(70,*) Y1,B1,Y2,B2,Y3,B3,Y4,B4
WRITE(60,30) Y1,A1,Y2,A2,Y3,A3,Y4,A4
40 CONTINUE
ENDIF
IF(ISW.EQ.3)THEN
WRITE(60,*)'C REPLACED Y OF ',SWdata,'by Y of ',PWdata
PRINT*, 'Replacing ',SWdata, 'AND ', PWdata
PRINT*, 'output file name is : ', TWdata
DO 50 I=1,6
CALL RDCMNT1
READ(80,*) X1,A1,X2,A2,X3,A3,X4,A4
CALL RDCMNT2
READ(70,*) Y1,B1,Y2,B2,Y3,B3,Y4,B4
WRITE(60,30) X1,B1,X2,B2,X3,B3,X4,B4
50 CONTINUE
ENDIF
STOP
END
```

```
C ——- SUBROUTINE TO READ COMMENT LINES IN THE DATA FILE
C ——- ALL COMMENT CARDS BEGIN WITH A 'C' OR A 'c'
SUBROUTINE RDCMNT1
INTEGER I
CHARACTER*72 DUMLIN

5 FORMAT(A)
DO 10 I = 1,100
READ(80,5) DUMLIN
IF ((DUMLIN(1:1).NE.'C').AND.(DUMLIN(1:1).NE.'c')) THEN
BACKSPACE ( UNIT = 80 )
GOTO 20
ENDIF
10 CONTINUE
20 CONTINUE
RETURN
END
C ————————————————————————————————————————-
SUBROUTINE RDCMNT2
INTEGER I
CHARACTER*72 DUMLIN
5 FORMAT(A)
DO 10 I = 1,100
READ(70,5) DUMLIN
IF ((DUMLIN(1:1).NE.'C').AND.(DUMLIN(1:1).NE.'c')) THEN
BACKSPACE ( UNIT = 70 )
GOTO 20
```

```
ENDIF
10 CONTINUE
20 CONTINUE
RETURN
END
C==================================================
```

APPENDIX B

The fraction of nominal contact area with increasing sliding time for the three tests.

Interval	Test S1	Test S2	Test S3
1	2.688	19.608	1.555
2	2.572	9.412	1.523
3	1.176	5.094	1.329
4	0.809	1.162	0.809
5	0.809	0.809	0.809
6	-	0.809	-

APPENDIX C

PWFTdata: Wear Rate of pin (W/ft) vs. Sliding Time

0 0 0 0 0 0 0 0

20 .0166 20 .1214 20 .0289 20 0

40 .0166 40 .1796 40 .0571 33 .0769

60 .0311 60 .2115 60 .0653 33 .0769

85 .0551 80 .2331 115 .0762 33 .0769

89 .2551 95 .3264 119 .4762 37 1.2269

89 .2551 99 1.0262 119 .4762 37 1.2269

SWFTdata: Spec Wear Rate (W/ft) vs. Sliding Time

0 0 0 0 0 0 0 0

20 .0332 20 .1214 20 0 20 0

40 .1445 40 .2960 40 .0471 33 .7923

60 .2314 60 .5192 60 .0965 33 .7923

85 .6474 80 .8209 115 .2274 33 .7923

89 2.992 95 1.9409 119 5.3774 37 11.8923

89 2.992 99 13.1524 119 5.3774 37 11.8923

TWFTdata: SUM of the data of SWFTdata and PWFTdata

0 0 0 0 0 0 0 0

20.000 0.050 20.000 0.243 20.000 0.029 20.000 0.000

40.000 0.161 40.000 0.476 40.000 0.104 33.000 0.869

60.000 0.262 60.000 0.731 60.000 0.162 33.000 0.869

85.000 0.703 80.000 1.054 115.000 0.304 33.000 0.869

89.000 3.247 95.000 2.267 119.000 5.854 37.000 13.119

89.000 3.247 99.000 14.179 119.000 5.854 37.000 13.119

PWFdata: Wear rate of pin (W/f) vs. sliding time

0 0 0 0 0 0 0 0

20 .3324 20 2.4272 20 .5770 20 0

40 .3324 40 3.5913 40 1.1419 33 1.0

60 .6222 60 4.2291 60 1.3067 33 1.0

85 1.2222 80 4.6601 115 1.9067 33 1.0

89 2.0222 95 6.0601 119 3.5067 37 5.6

89 2.0222 99 8.2601 119 3.5067 37 5.6

SWFdata: spec wear Rate (W/f) vs. Sliding Time

0 0 0 0 0 0 0 0

20 .6649 20 2.4272 20 0 20 0

40 2.8914 40 5.9196 40 .9414 33 10.3

60 4.63 60 10.3839 60 1.9302 33 10.3

85 15.030 80 16.4175 115 9.1302 33 10.3

89 24.1300 95 33.2175 119 29.7302 37 54.7

89 24.1300 99 64.3175 119 29.7302 37 54.7

TWFdata: SUM of the data of SWFdata and PWFdata

0 0 0 0 0 0 0 0

20.000 0.997 20.000 4.854 20.000 0.577 20.000 0.000

40.000 3.224 40.000 9.511 40.000 2.083 33.000 11.300

60.000 5.252 60.000 14.613 60.000 3.237 33.000 11.300

85.000 16.252 80.000 21.078 115.000 11.037 33.000 11.300

89.000 26.152 95.000 39.278 119.000 33.237 37.000 60.300

89.000 26.152 99.000 72.578 119.000 33.237 37.000 60.300

PWTdata: Wear Rate of pin (W/T) vs. sliding time

0 0 0 0 0 0 0 0

20 .005 20 .005 20 .015 20 0

40 .005 40 .01 40 .030 33 .0769

60 .015 60 .015 60 .035 33 .0769

85 .039 80 .030 115 .0459 33 .0769

89 .2390 95 .1233 119 .4459 37 1.2269

89 .2390 99 .6733 119 .4459 37 1.2269

SWTdata: Spec Wear rate vs. sliding time (W/t vs. T)

0 0 0 0 0 0 0 0

20 .010 20 .005 20 0 20 0

40 .045 40 .02 40 .025 33 .7923

60 .105 60 .055 60 .055 33 .7923

85 .5210 80 .2650 115 .1859 33 .7923

89 2.7960 95 1.3850 119 5.3359 37 11.8923

89 2.7960 99 9.1600 119 5.3359 37 11.8923

TWTdata: SUM of the data of SWTdata and PWTdata

0 0 0 0 0 0 0 0

20.000 0.015 20.000 0.010 20.000 0.015 20.000 0.000

40.000 0.050 40.000 0.030 40.000 0.055 33.000 0.869

60.000 0.120 60.000 0.070 60.000 0.090 33.000 0.869

85.000 0.560 80.000 0.295 115.000 0.232 33.000 0.869

89.000 3.035 95.000 1.508 119.000 5.782 37.000 13.119

89.000 3.035 99.000 9.833 119.000 5.782 37.000 13.119

PWdata: Wear rate of specimen with time (w vs t)

0 0 0 0 0 0 0 0

20 .2 20 0.1 20 0 20 0

40 .9 40 .4 40 .5 33 10.3

60 2.1 60 1.1 60 1.1 33 10.3

85 12.5 80 5.3 115 8.3 33 10.3

89 21.6 95 22.1 119 28.9 37 54.7

89 21.6 99 53.2 119 28.9 37 54.7

SWdata: Wear rate of pin (w) with time

0 0 0 0 0 0 0 0

20 .1 20 .1 20 .3 20 0

40 .1 40 .2 40 .6 33 1.0

60 .3 60 .3 60 .7 33 1.0

85 .9 80 .6 115 1.3 33 1.0

89 1.7 95 2.0 119 2.9 37 5.6

89 1.7 99 4.2 119 2.9 37 5.6

TWdata: SUM of the data of SWdata and PWdata

0 0 0 0 0 0 0 0

20.000 0.300 20.000 0.200 20.000 0.300 20.000 0.000

40.000 1.000 40.000 0.600 40.000 1.100 33.000 11.300

60.000 2.400 60.000 1.400 60.000 1.800 33.000 11.300

85.000 13.400 80.000 5.900 115.000 9.600 33.000 11.300

89.000 23.300 95.000 24.100 119.000 31.800 37.000 60.300

89.000 23.300 99.000 57.400 119.000 31.800 37.000 60.300

APPENDIX D

The data for lubricated wear tests (Comparative wear tests) C Piston ring wear rate data in volume loss with increasing load, under lubrication

10 .060 .013 .005

20 .097 .030 .030

40 .089 .241 .239

C Specimen wear rate data in volume loss with increasing load, under lubrication

10 .115 .03 .022

20 .270 .072 .06

40 .459 .120 .079

C Total wear rate data in volume loss with increasing load, under lubrication

10 .175 .043 .027

20 .367 .102 .090

40 .548 .361 .318